Experimental study on the flow and heat transfer characteristics of nanofluids in double-tube heat exchangers based on thermal efficiency assessment

Cong Qi [a, b, c, *], Tao Luo [a, b], Maoni Liu [a, b], Fan Fan [a, b], Yuying Yan [c]

[a] Jiangsu Province Engineering Laboratory of High Efficient Energy Storage Technology and Equipments, China University of Mining and Technology, Xuzhou 221116, China

[b] School of Electrical and Power Engineering, China University of Mining and Technology, Xuzhou 221116, China

[c] Fluids & Thermal Engineering Research Group, Faculty of Engineering, University of Nottingham, Nottingham NG7 2RD, UK

Abstract: Thermal performance and pressure drop of TiO_2-H_2O nanofluids in double-tube heat exchangers are investigated. The influence of the thermal fluid (water) volume flow rates (q_v=1-5L/min), nanoparticle mass frictions (ω=0.0%, 0.1%, 0.3% and 0.5%), nanofluids locations (shell-side and tube-side), Reynolds numbers of nanofluids (Re=3000-12000), and the structures of inner tubes (smooth tube and corrugated tube) is analyzed. Results indicate that nanofluids (ω=0.1%, 0.3% and 0.5%) can improve the heat transfer rate by 10.8%, 13.4% and 14.8% at best compared with deionized water respectively, and the number of transfer units (NTU) and effectiveness are all improved. The pressure drop can be increased by 51.9% (tube-side) and 40.7% (shell-side) at best under the condition of using both nanofluids and corrugated inner tube. When the nanofluids flow in the shell-side of the corrugated double-tube heat exchanger, the comprehensive performance of nanofluids-side is better than that of the smooth double-tube heat exchanger.

Key words: Nanofluids; Double-tube heat exchanger; Thermal efficiency; Heat transfer enhancement

[*]Correspondence author.
E-mail: qicong@cumt.edu.cn (C. Qi); luotao@cumt.edu.cn (T. Luo); liumaoni@cumt.edu.cn (M. Liu); fanfan@cumt.edu.cn (F. Fan); yuying.yan@nottingham.ac.uk (Y. Yan)

Nomenclature

A	heat transfer surface area, m^2
c_p	specific heat, $J \cdot kg^{-1} \cdot K^{-1}$
d	equivalent diameter, m
f	the frictional resistance coefficient
h	the overall heat transfer coefficient, $W/m^2 K$
L	length of tube, m
m	the mass flow rate of the hot water, kg/s
NTU	number of transfer units
P	pressure, Pa
ΔP	pressure drop, Pa
q_v	the volume flow rate of the hot water, L/min
Q	the heat transfer rate, W
Re	Reynolds number
T	the fluid temperature, K
ΔT_m	the logarithmic mean temperature difference, K
u	velocity, m/s
Greek symbols	
δ	wall thickness of tube, m
ε	effectiveness
ρ	density, kg/m^3
ω	mass fraction
Subscripts	
ave	average
in	inlet
min	minimum
max	maximum
nf	nanofluids
out	outport
w	thermal water

1 Introduction

Nanofluids, as heat transfer medium, have been applied into various fields because of their excellent thermal performance. Many investigators not only measured the thermal conductivity [1, 2, 3], but also developed some empirical formulas of thermal conductivity [4, 5, 6, 7], a more detailed review of the research on the preparation methods and thermal property parameters of nanofluids can be found in the literature [8]. Furthermore, for the practical application of nanofluids, a guideline for the selection of nanofluids has also been studied [9]. The application fields of nanofluids mainly including full-spectrum photo-thermal conversion [10, 11], tunable and recyclable photovoltaic/thermal applications [12, 13], vapor generation by different nanoparticles or nanofluids (Fe_3O_4@CNT nanoparticles [14], carbon-nanotube nanofluids [15], graphene oxide nanofluids [16] and MCE/HP/Au mixed nanoparticles [17]), boiling heat transfer [18], thermal energy storage [19, 20], CPU cooling [21, 22, 23, 24], microchannel [25, 26], heat pipe [27, 28], and so on.

In the field of heat exchange equipment, there are two crucial heat transfer methods: free convection and forced convection. For free convection, lots of researches have been reported by published literatures. Shi et al. [29] performed an investigation on the free convection of Fe_3O_4@CNT nanofluids in a rectangular cavity under magnetic field conditions using experimental and numerical simulation methods. Results indicated that the direction of magnetic field can regulate the thermal performance of nanofluids. Selimefendigil et al. reported on a numerical method which was used to study the free convection of CNT-water nanofluids in a two-dimension enclosure with corrugated partition [30] and three kinds of nanofluids in a three dimensional cavity with rotating circular cylinders [31] respectively. It was discovered that the thermal performance of nanofluids decreases with the height of the triangular waves in the two-dimension enclosure, and the rotational direction of circular cylinders also has a significant role in heat transfer. Sajjadi et al. [32] represented a numerical simulation study on the free convection of MWCNT-Fe_3O_4/water nanofluids in a square cavity full of porous media. Results showed that the increasing Darcy number and porosity can enhance the thermal performance. The natural convection of nanofluids in various cavities is widely researched. For example, nanofluids in an inclined cavity [33], an open cavity [34], an open inclined cavity [35], a cavity with a heat-generating element [36], a tilted porous cavity [37], a baffled U-shaped enclosure [38], a three dimensional porous cavity [39], a annular cavity filled with porous media under electric field [40], a semi annulus [41], and a square cavity full of a porous foam [42]. The influence of Rayleigh number, nanoparticle concentration, porous layer, cavity inclination angle, heat source location, and cavity aspect ratio on the thermal performance was analyzed. Results presented that nanofluids have more excellent heat transfer compared with base fluid.

Also, many studies have been conducted on the forced convection. Xu et al. [43] reported on a numerical simulation method which was obtained to study the flow and thermal performances of Al_2O_3-H_2O nanofluids flowing through a channel filled with Cu metal-foam. It was obtained that thermal performance of nanofluids in metal foam is effectively improved at the expense of a large increase in pressure drop. Mohebbi et al. [44] adopted a lattice Boltzmann method to research the forced convection of three kinds of nanofluids (CuO, Al_2O_3 and TiO_2) flowing through a channel with blocks at the top and bottom of wall. Conclusions indicated that as the space between the blocks decreases, the thermal performance increases. Karimi et al. [45] applied MgO-MWCNTs/EG nanofluids into heat exchanger, and results indicated that nanofluids with concentration 1% can improve the thermal performance by 20%, but the pressure drop also increases. Tirandaz et al. [46] performed a numerical investigation to research the forced convection in a helical annulus filled with a porous medium. And two different boundary conditions is considered. Conclusions indicated that the Nusselt number is insensitive to the second-order torsion of the dimensionless curvature, and the enhancement of the Nusselt number is more pronounced at higher curvature values. Mehrali et al. [47] performed an experimental study on the thermal performance and flow characteristic of grapheme nanoplatelet nanofluids in a stainless steel tube, and obtained that the thermal performance of nanofluids can be improved by 83-200% compared with base fluid. In addition to the analysis of quantity of energy, Mehrali et al. [48, 49] also investigated the entropy generation of nanofluids under forced flow from the quality. Moradikazerouni et al. [50] carried out a numerical method to investigate the convection performance of γ-AlOOH nanofluids in a wavy channel, and explore the influence of the Reynolds number, amplitude of wavy channel and nanoadditive fraction. Mirzaei et al. [51] investigated the thermal performance of Al_2O_3-H_2O nanofluids under laminar flow in micro channel and obtained that the influence of the variable is obviously, and the influence of temperature variation on thermal performance cannot be neglected. Sun et al. researched the thermal performance of nanofluids in an external thread tubes which own a built-in twisted belt [52], plate heat exchanger [53], and copper tubes [54] respectively. Results proved that Reynolds number and nanoparticle concentration are all positive factors for the thermal performance improvement. Sheikholeslami et al. carried out a study on the heat exchanger enhancement and flow characteristics of nanofluids in a double-tube heat exchanger [55], a porous semi annulus [56], a porous lid driven cubic cavity [57], a three dimension square cavity [58], and an annular cavity [59, 60], explored the influence of nanoparticle fraction and magnetic field on thermal exchange, and found that these factors can effectively improve the thermal performance. Ranjbarzadeh et al. [61] carried out an empirical analysis method to investigate the thermal performance and flow characteristic of nanofluids in an isothermal pipe under forced convection condition. Results showed that nanofluids can improve the thermal performance by 40.3% compared with base fluid. Moradikazerouni et al. [62] studied the influence of the entrance channel shapes on the heat transfer enhancement in a micro-channel heat sink using a numerical method, and results showed that the triangular shape provides the best thermal performance in the five channel configurations. Dehghan et al. [63] represented an investigation on the thermal performance in microchannels enhanced by porous materials and obtained that the comprehensive evaluation of heat transfer and pressure drop can be effectively enhanced by inserting a thin porous insert. Dehghan et al. [64] also investigated the influence of Al_2O_3-water nanofluids on the forced convection in a microchannel heat sink using a numerical simulation. Nojoomizadeh et al. [65] carried out an numerical method to explore the effects of permeability on the forced convection of nanofluids in a micro channel, the investigation indicated that the thermal performance increases with the decreasing permeability. Moradikazerouni et al. [66] reported a numerical simulation method which was used to study the influence of laminar forced convection on the heat transfer enhancement in a CPU heat sink, compared with convection-radiation, the pure convection has less thermal performance improvement. Ranjbarzadeh et al. [67] represented an experimental investigation on the forced convection of nanofluids in a copper tube and obtained that Nusselt number can be increased by 51.4% compared with water. Biglarian et al. [68] reported on a study to explore the forced convection of various nanofluids (Cu, Ag, Al_2O_3, TiO_2) and obtained that Cu nanofluids show the largest enhancement ratio. Many enhanced tubes and nanofluids are applied to enhance the thermal performance. Naphon et al. reported an investigation on the thermal performance and pressure drop of nanofluids in a helically corrugated tube [69], a micro-fins tube [70], a spirally coiled tube [71], and a micro-channel heat sink [72]. Qi et al. also did lots of work in enhanced tubes, for example, spiral tubes [73], corrugated tubes [74, 75, 76], triangular tubes [77, 78], a circular tube with rotating twisted [79], a horizontal elliptical tube [80]. From above references, it was found that nanofluids can all improve the thermal performance at the expense of a significant increase in pressure drop. Therefore, scholars have also done some work on the comprehensive assessment of the heat transfer enhancement and flow resistance [81, 82, 83].

From above studies, researchers mainly focus on the flow characteristic and thermal performance of nanofluids in a single enhanced tube. However, there are few published literatures on the application of nanofluids and enhanced tube into double-tube heat exchanger. The research proposal of this paper is to study the thermal performance and pressure drop of TiO_2-H_2O nanofluids in the corrugated double-tube heat exchanger using experimental method, and the innovations are as follows: Corrugated tube is applied in the tube-side instead of smooth tube; Effects of nanofluids location, nanoparticle mass fraction and thermal fluid flow rate on the thermo-hydraulic performances of nanofluids in the double-tube heat exchanger are investigated based on thermal efficiency assessment; The effectiveness and the *NTU* of double-tube heat exchanger are analyzed.

2 Experimental Method

2.1 Nanofluids preparation and stability

In this experiment, TiO_2 nanoparticle and deionized water (base fluid) are selected to prepare TiO_2-H_2O nanofluids with mass fractions (ω=0.0wt%, 0.1wt%, 0.3wt% and 0.5wt %) using two-step method. The preparation process is as follows: Firstly, TDL-ND1 dispersant is added into the deionized water while stirring the mixture fluid with a mechanical stirrer. TiO_2 nanoparticles are then added to the mixed solution, and NaOH solutions are also added to adjust the pH of the mixed solution to 8, at the same time, both mechanical and magnetic are used to stir in order to fully disperse the particles in the mixed solution. Finally, ultrasonic vibration is applied to the mixed solution using an ultrasonic vibrometer. So TiO_2-H_2O nanofluids are obtained.

Although nanofluids have better heat transfer enhancement effects, the stability and economics of nanofluids are currently the main problems and shortcomings. Hence, the details on the stability and thermophysical parameters of TiO_2-H_2O nanofluids have been investigated in previous published reference [80]. The prepared nanofluids have good stability after standing for 20 days.

2.2 Experimental system

The schematic diagram and the real experimental setup of the corrugated double-tube heat exchanger experimental setup are shown in Fig. 1 and Fig. 2 respectively. The experimental setup consists of a test section, a low-temperature thermostat bath, a hot water tank, two pumps, two valves, two flow meters and collection tanks. The inner tube (corrugated tube) in test section is made of stainless steel with D_{max}=15.8mm and D_{min}=11.2mm, the wall thickness is δ=0.25mm, while the outer shell is made of PVC with 32mm outer diameter and 28mm inner diameter. The total length of double-tube heat exchanger is 1200mm. Insulating layer covered on the outer tube is adopted to prevent the heat loss. There are two working fluids including thermal fluid (deionized water) and cold fluid (TiO_2-H_2O nanofluids) in the two circulation closed units. The pressure drop and temperatures of the thermal fluid and nanofluids are measured by differential pressure transmitters (type: MIK-3051, pressure measuring range: 0-1KPa and 0-5KPa) and four thermocouples, which are installed in the import and export of the heat exchanger. A date acquisition instrument (type: 34972A, manufacturer: Agilent) is used to collect the temperature date.

Furthermore, a low-temperature thermostat bath (type: DC-2030A, accuracy: ±0.05 ℃) is adopted to keep the cold fluids (nanofluids) temperature constant, and the thermal fluid (deionized water) temperature is regulated by a hot water tank with a thermostat (type: DC-2030A, accuracy: ±0.05 ℃). And the smooth double-tube heat exchanger only has the difference of inner tube type. In addition, the boundary conditions of the experiments are shown in Table 1.

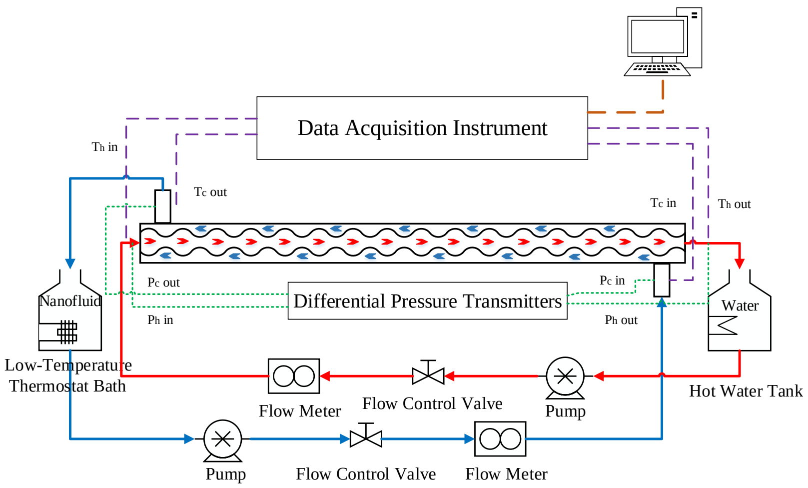

Fig. 1. Schematic diagram of the experimental system

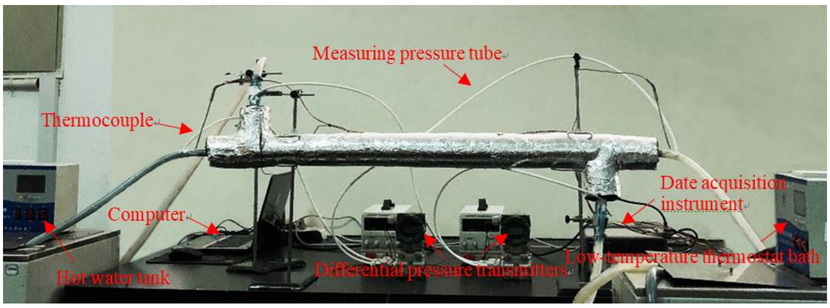

Fig. 2. The experimental system of the corrugated double-tube heat exchanger

The experimental procedure is as follows:

(1) Place the nanofluids in the low-temperature thermostat bath and deionized water in the hot water tank, and set the temperature to the desired value.

(2) Open the all valves, flow meters and pumps of the experimental system, two kinds of working fluids begin to circulate in the two loops, and carefully check the

experimental system for leakage.

(3) Open the differential pressure transmitters, date acquisition instrument and computer, collect date of the import and export of the two loops, perform more than three experiments on each experimental condition and record the experimental dates.

(4) When the experiment is completed, turn off the high-power thermostat, then turn off the pumps and date acquisition instrument, finally turn off the main power.

Table 1 Boundary conditions of the experiment

Type	Nanofluids in tube-side		Nanofluids in shell-side	
Inlet Temperature	20 ℃ (tube-side)	40 ℃ (shell-side)	40 ℃ (tube-side)	20 ℃ (shell-side)
Range	*Re* 3000-12000	q_v 1-5 L/min	q_v 1-5 L/min	*Re* 3000-12000
Outer wall (shell)	Insulation wall			
Outer wall (tube)	Heat transfer surface			

2.3 Experimental data processing

The average heat exchange capacity from thermal fluid (deionized water) to cold fluid (nanofluids) is defined as:

$$Q_{\mathrm{ave}} = \frac{Q_{\mathrm{w}} + Q_{\mathrm{nf}}}{2} \tag{1}$$

where

$$Q_{\mathrm{w}} = m_{\mathrm{w}} c_{\mathrm{pw}} (T_{\mathrm{in}} - T_{\mathrm{out}})_{\mathrm{w}} \tag{2}$$

$$Q_{\mathrm{nf}} = m_{\mathrm{nf}} c_{\mathrm{pnf}} (T_{\mathrm{out}} - T_{\mathrm{in}})_{\mathrm{nf}} \tag{3}$$

The logarithmic mean temperature difference ΔT_{m} is evaluated from:

$$\Delta t_{\mathrm{m}} = \frac{\Delta t_{\max} - \Delta t_{\min}}{\ln \frac{\Delta t_{\max}}{\Delta t_{\min}}} \tag{4}$$

The overall heat transfer coefficient is expressed as:

$$h = \frac{Q_{\text{ave}}}{A\Delta T_{\text{m}}} \tag{5}$$

The effectiveness and the *NTU* are given by:

$$NTU = \frac{hA}{(mc)_{\min}} \tag{6}$$

$$\varepsilon = \frac{1-\exp\left\{(-NTU)[1-\frac{(mc)_{\min}}{(mc)_{\max}}]\right\}}{1-\frac{(mc)_{\min}}{(mc)_{\max}}\exp\left\{(-NTU)[1-\frac{(mc)_{\min}}{(mc)_{\max}}]\right\}} \tag{7}$$

The frictional resistance coefficient can be calculated with:

$$f = \frac{2d}{\rho u^2}\cdot\frac{\Delta P}{L} \tag{8}$$

3 Results and discussions

3.1 Experimental system validation

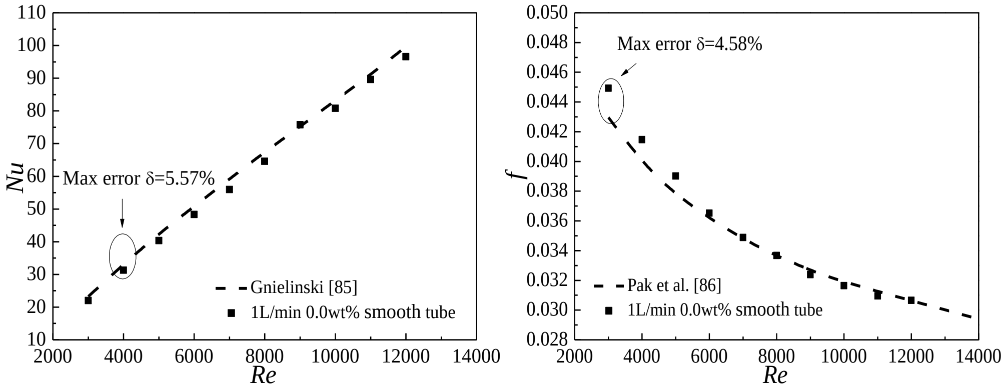

Fig. 3. Comparison between the experimental results and other results in published references, (a) *Nu*, (b) *f*

Before beginning to study the characteristics of the thermal performance and pressure drop, an analysis of the reliability and accuracy of the experimental setup is required. Nusselt number are obtained using "Wilson plots" method [84], and the comparison of the Nusselt number between this experiment and the published reference [85] is shown in Fig 3(a). It can be found that the experimental results are in good agreement with the published reference, and the maximum difference between them is around 5.57%. Fig. 3 also shows the resistance coefficient comparison between this experiment and published reference [86]. Results show that the errors are within 4.58%. The above studies can verify the reliability and accuracy of this experimental system.

3.2 Error analysis

Based on the root-sum-square method presented by Kline [87], the errors of physical parameters can be calculated from following equations (9-11), and the results are shown in Table 2. It is indicated that the maximum uncertainties in the resistance coefficient, *NTU* and effectiveness are ±1.18%, ±1.77%, and ±2.06% respectively.

$$\frac{\delta NTU}{NTU}=\sqrt{\left(\frac{\delta Q}{Q}\right)^2+\left(\frac{\delta l}{l}\right)^2+\left(\frac{\delta m}{m}\right)^2+\left(\frac{\delta T}{T}\right)^2} \tag{9}$$

$$\frac{\delta \varepsilon}{\varepsilon}=\sqrt{\left(\frac{\delta NTU}{NTU}\right)^2+\left(\frac{\delta m}{m}\right)^2} \tag{10}$$

$$\frac{\delta f}{f}=\sqrt{\left(\frac{\delta \Delta p}{\Delta p}\right)^2+\left(\frac{\delta l}{l}\right)^2+\left(\frac{\delta m}{m}\right)^2} \tag{11}$$

Table 2 Errors of each section in the experiment

$\delta Q/Q$	$\delta T/T$	$\delta\Delta p/\Delta p$	$\delta l/l$	$\delta m/m$	$\delta NTU/NTU$	$\delta\varepsilon/\varepsilon$	$\Delta f/f$
±1.0%	±1.0%	±0.5%	±0.1%	±1.06%	±1.77%	±2.06%	±1.18%

3.3 Experimental results and discussions

3.3.1 Shell-side water and tube-side nanofluids

In the experimental study of the smooth and corrugated double-tube heat exchangers, the heat transfer medium in tube-side is TiO_2-H_2O nanofluids with different mass fractions ω=0.0%, 0.1%, 0.3% and 0.5%, and the inlet temperature is 20°C. The shell-side working fluid is the thermal fluid (deionized water) with an inlet temperature of 40°C. The Reynolds numbers of the nanofluids range from 3000 to

12000, and the thermal fluid volume flow rates range from 1L/min to 5L/min in this experiment.

3.3.1.1 Heat transfer rate

Fig. 4 and Fig. 5 show the influence of Nanofluids mass fraction on the heat transfer rate of smooth and corrugated double-tube heat exchangers, and Fig. 6 is a summary graph on the heat transfer rate changes with velocity.

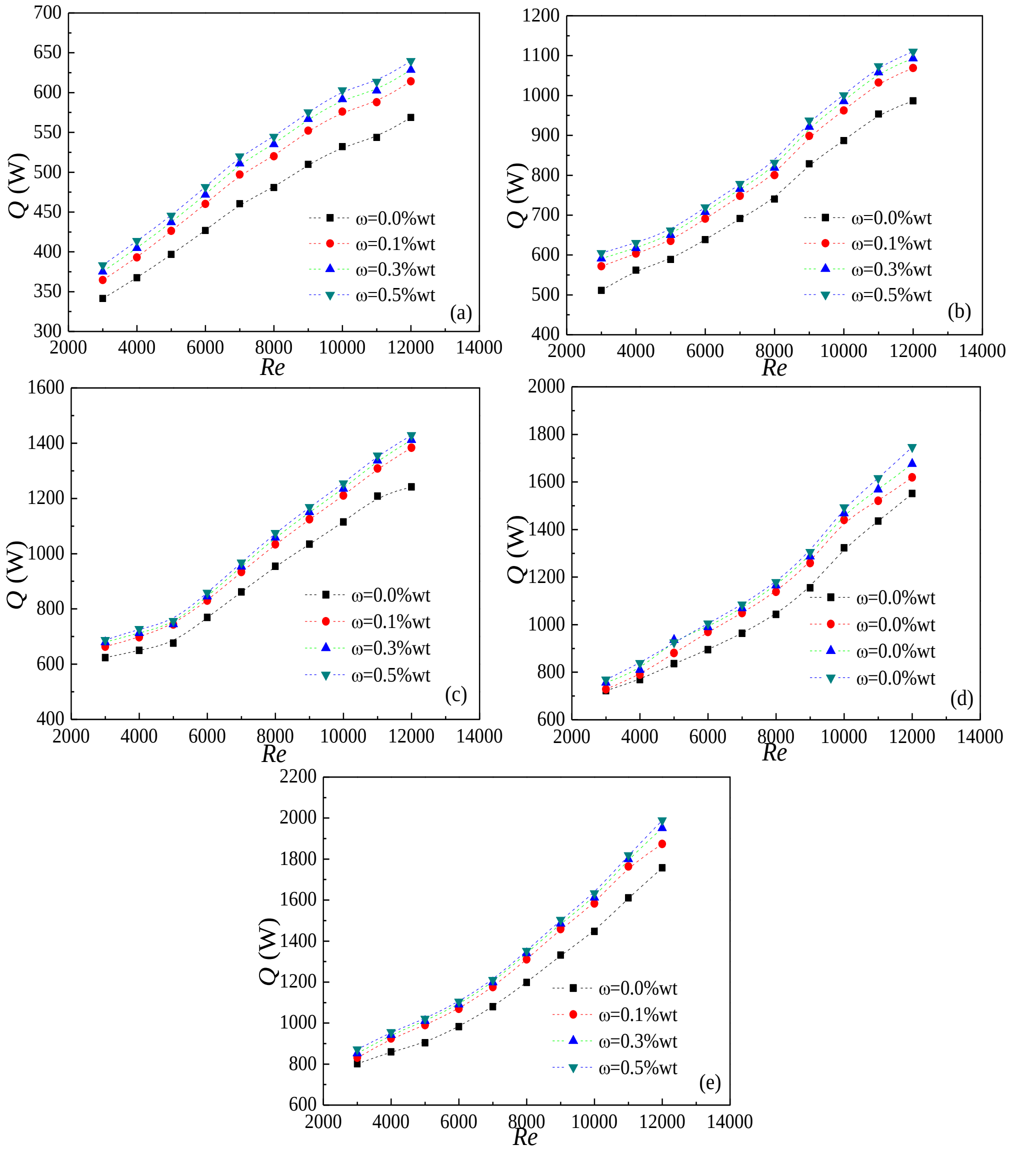

Fig. 4. Effects of nanoparticle mass fraction on the heat transfer rate of the smooth double-tube heat exchanger, (a) q_v=1L/min, (b) q_v=2L/min, (c) q_v=3L/min, (d) q_v=4L/min, (e) q_v=5L/min

It is indicated that the increase of Reynolds number (velocity) promotes the improvement of the heat transfer rate, and using both the nanofluids and corrugated tube can effectively improve the heat transfer rate. In the corrugated double-tube heat exchanger, the heat transfer rate with ω=0.1%, 0.3%, 0.5% can be improved by 10.8%, 13.4% and 14.8% at best compared with deionized water respectively. There are two main reasons to explain this enhancement. Nanofluids have greater thermal conductivity than deionized water, also nanofluids have stronger Brownian motion compared to deionized water [88].

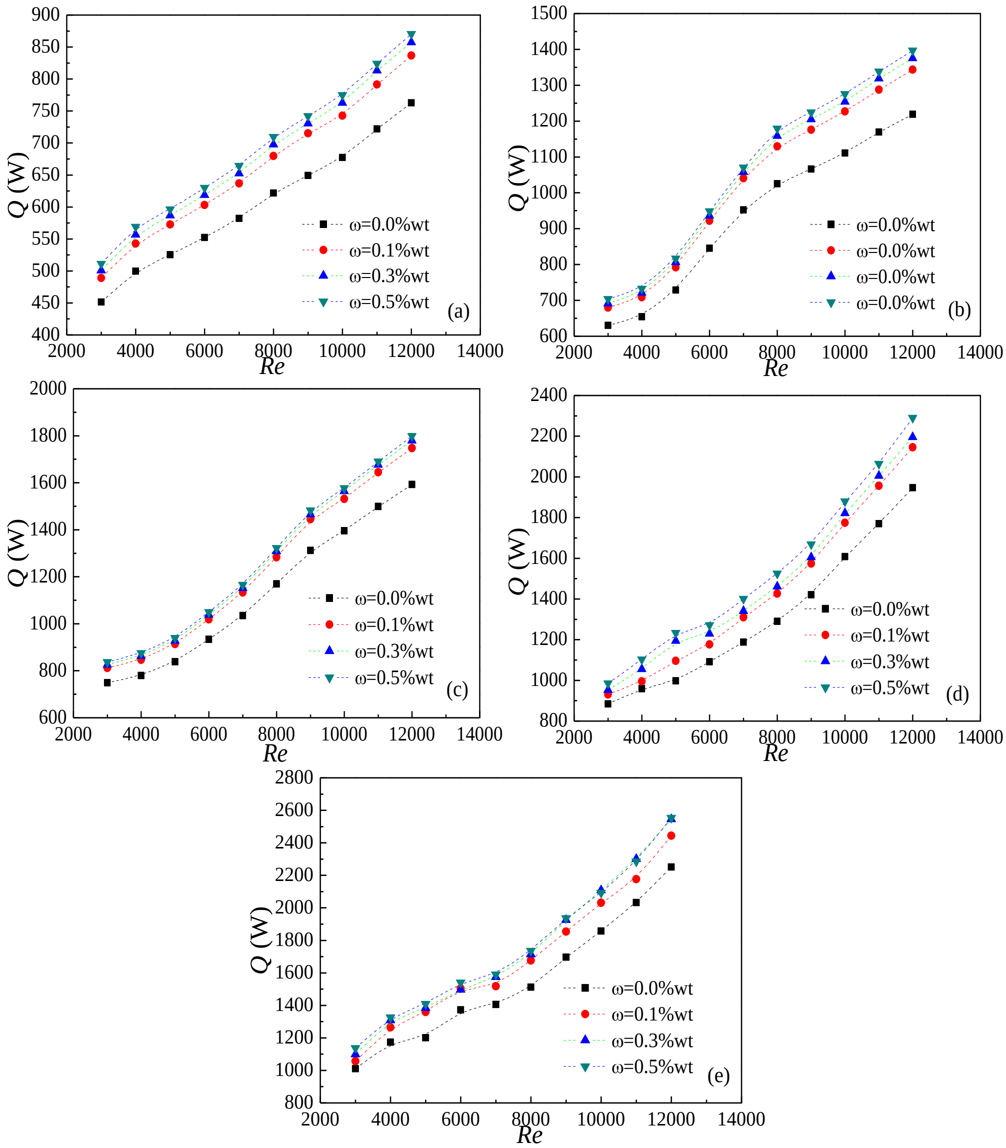

Fig. 5. Effects of nanoparticle mass fraction on the heat transfer rate of the corrugated double-tube heat exchanger, (a) q_v=1L/min, (b) q_v=2L/min, (c) q_v=3L/min, (d) q_v=4L/min, (e) q_v=5L/min

The effects of the thermal fluid volume flow rates are also showed in Figs. 4-6. It is indicated that the increase of thermal fluid flow rate promotes the increase of the heat transfer rate. However, the enhanced heat transfer capacity of nanofluids shows slightly larger compared with deionized water when the thermal fluid flow rates are larger. The heat transfer rate of nanofluids is improved slightly with the increase of the thermal fluid flow rate.

In the smooth double-tube heat exchanger, take ω=0.1% as an example, the heat transfer rate can be improved by 8.29%, 8.56%, 8.7%, 9.13% and 9.49% at best compared with deionized water when the volume flow rates range from 1L/min to 5L/min. Furthermore, Figs. 4-6 also manifest that the improvement in heat transfer rate is more pronounced as the increasing thermal fluid flow rate, which causes more efficient heat transfer between the nanoparticles and the inner tube surface, but the increase is not large. And when the volume flow rates range from 1L/min to 5L/min, the heat transfer rate of the corrugated double-tube heat exchanger can be improved by 9.76%, 10.16%, 10.31%, 10.64% and 10.88% at best compared with deionized water, which indicates that the disturbing effect of the corrugated tube also increases the probability of mutual collision between the nanoparticles, so that the thermal performance is further strengthened.

Comparison of the heat transfer rate between two kinds of heat exchangers can be also obtained from Figs. 4-6. The heat transfer rate is much better in the corrugated double-tube heat exchanger, and it can be improved by 47.1% at best under the same condition.

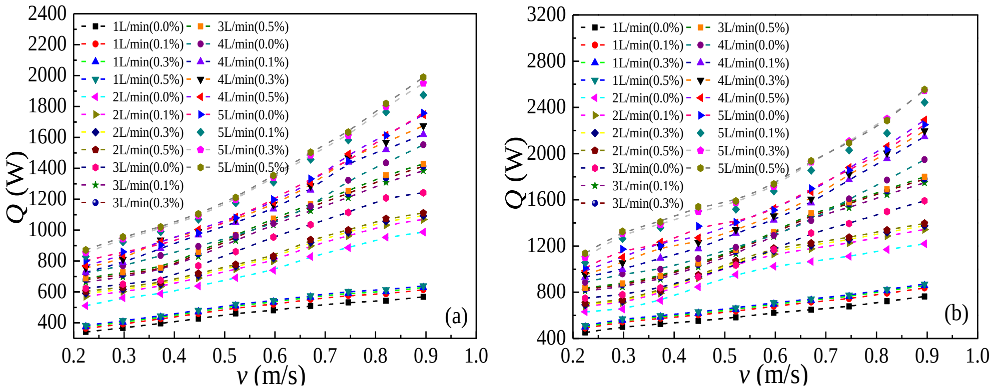

Fig. 6. The summary graph on the heat transfer rate with velocity, (a) smooth tube, (b) corrugated tube

3.3.1.2 *NTU*

In a heat exchanger, the main indexes for the thermal performance are the number of transfer units (*NTU*) and effectiveness. Hence, the two enhancement indexes will be analyzed and discussed in the following section.

Fig. 7 and Fig. 8 show the variations of *NTU* in the smooth and corrugated double-tube heat exchangers, and Fig. 9 is a summary graph on *NTU* with velocity. As displayed in Fig. 7 and Fig. 8, the trends of the *NTU* are more diverse compared with Fig. 4 and Fig. 5. *NTU* shows the effects of the relationship between the flow rates of the thermal fluid and cold fluid on the overall thermal performance of the heat exchanger, so its value is also related to the relative flow rates of the two kinds of working fluids.

When the thermal fluid flow rates are 1L/min and 2L/min, as the Reynolds number increases, the *NTU* of the two kinds of double-tube heat exchangers all increases. But when volume flow rates are from 3L/min to 5L/min, the *NTU* shows a trend of decreasing firstly and then increases. This phenomenon can be explained by formula (6). From formula (6), it can be found that the *NTU* is related to the minimum flow rates of the nanofluids and thermal fluid. The thermal fluid flow rate in the downward trend is smaller than the cold fluid flow rate, and in the upward trend, the cold fluid flow rate is greater than the thermal fluid flow rate, in theory, the lowest point occurs when the two fluids flow rate are the same. And as displayed in Figs. 7-8 (c), (d) and (e), as the flow rate of thermal fluid increases, the *NTU* shows a downward trend and the lowest point also moves toward the high Reynolds number.

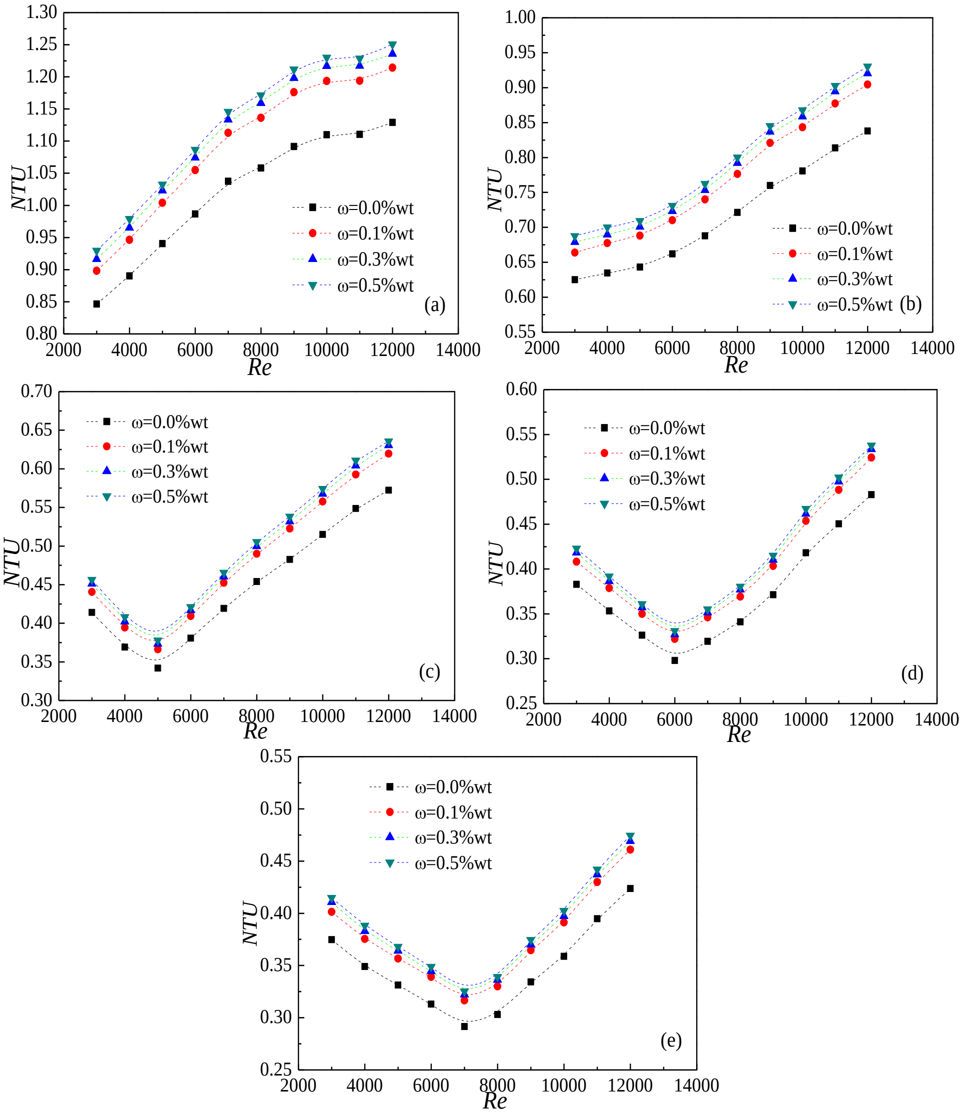

Fig. 7. Effects of nanoparticle mass fraction on *NTU* of the smooth double-tube heat exchanger, (a) q_v=1L/min, (b) q_v=2L/min, (c) q_v=3L/min, (d) q_v=4L/min, (e) q_v=5L/min

Furthermore, with the increase of the nanofluids mass fraction, the *NTU* also increases correspondingly, which indicates that nanofluids can improve the heat exchange capacity of heat exchangers. The *NTU* of the corrugated double-tube heat exchanger with ω=0.1%, 0.3%, 0.5% can be improved by 10.7%, 12.6% and 13.6% at best compared with deionized water respectively. Comparative analysis of the *NTU* in the two kinds of heat exchangers can be also obtained from Figs. 7-9, the *NTU* of the corrugated double-tube heat exchanger is higher, and it can be improved by 47.5% at best under the same condition.

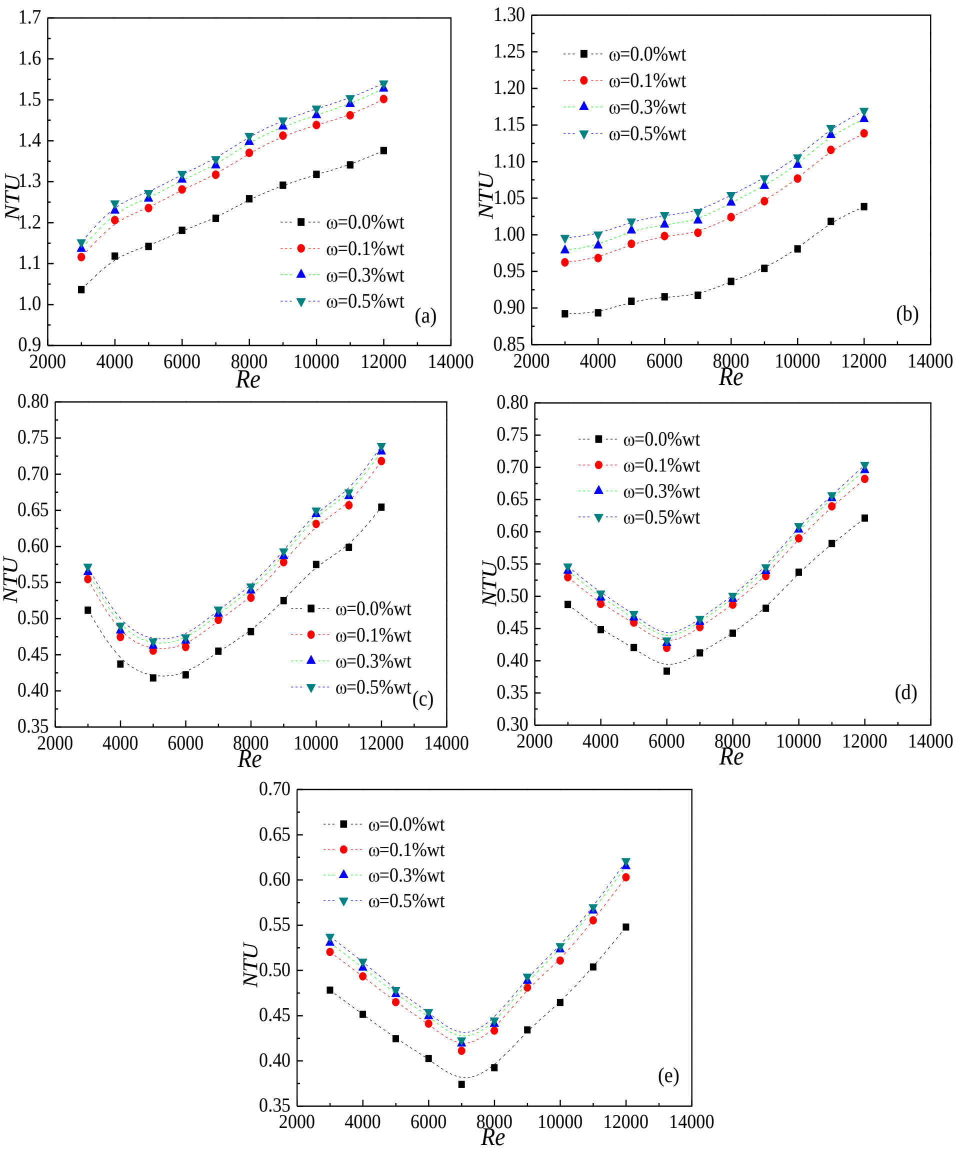

Fig. 8. Effects of nanoparticle mass fraction on *NTU* of the corrugated double-tube heat exchanger, (a) q_v=1L/min, (b) q_v=2L/min, (c) q_v=3L/min, (d) q_v=4L/min, (e) q_v=5L/min

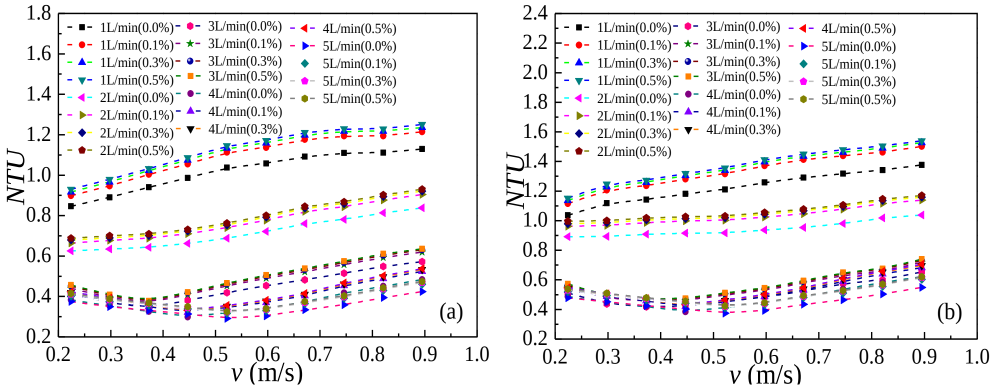

Fig. 9. The summary graph on the *NTU* with velocity, (a) smooth tube, (b) corrugated tube

3.3.1.3 Effectiveness

Effectiveness shows a similar trend with *NTU*. Fig. 10 and Fig. 11 show the influence of nanofluids mass fraction and the thermal fluid volume flow rates on the effectiveness of the smooth and corrugated double-tube heat exchangers respectively, and Fig. 12 is a summary graph on effectiveness changes with velocity. It is indicated that when the thermal fluid flow rate is larger, the effectiveness decreases, which means that when the Reynolds number of nanofluids is constant, increasing the thermal fluid volume flow rate can improve the heat transfer rate, but it does not necessarily improve the effectiveness. This phenomenon can make the industry to obtain the actual thermal performance required by adjusting the flow rates of thermal fluid and nanofluids.

Under the strengthening effect of nanofluids, the effectiveness of the two kinds of double-tube heat exchangers has been improved. Taking the thermal fluid in shell-side with a volume flow rate of 5L/min and a Reynolds number of 9000 in tube-side as an example, it can be found that TiO_2-H_2O nanofluids with ω=0.1%, 0.3% and 0.5% can improve the effectiveness from 31.1% to 33.4%, 33.8% and 34.1% respectively compared with deionized water.

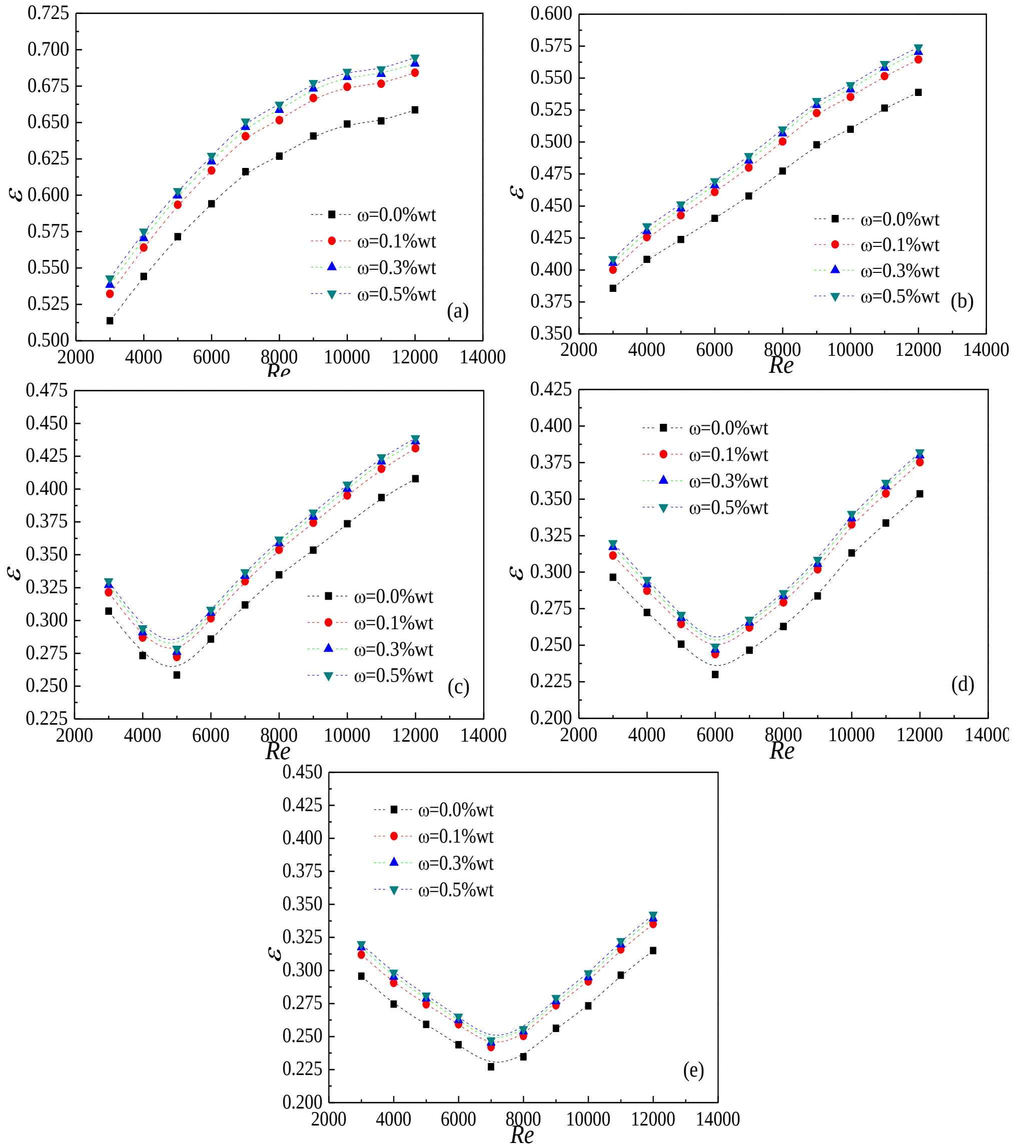

Fig. 10. Effects of nanoparticle mass fraction on the effectiveness of the smooth double-tube heat exchanger, (a) q_v=1L/min, (b) q_v=2L/min, (c) q_v=3L/min, (d) q_v=4L/min, (e) q_v=5L/min

At the same time, this section takes the volume flow rates (from 1L/min to 5L/min) in shell-side and a Reynolds number of 9000 in tube-side as an example, The intuitive comparative analysis on the effectiveness in the smooth and corrugated double-tube heat exchangers is studied. Compared with deionized water in the smooth double-tube heat exchanger, the effectiveness of nanofluids in the corrugated double-tube heat exchanger is improved from 64.1%, 49.8%, 35.3%, 28.3%, 25.6% to 73.8%, 61.2%, 40.9%, 37.5%, 34.1% respectively. It is obtained that the nanoparticles

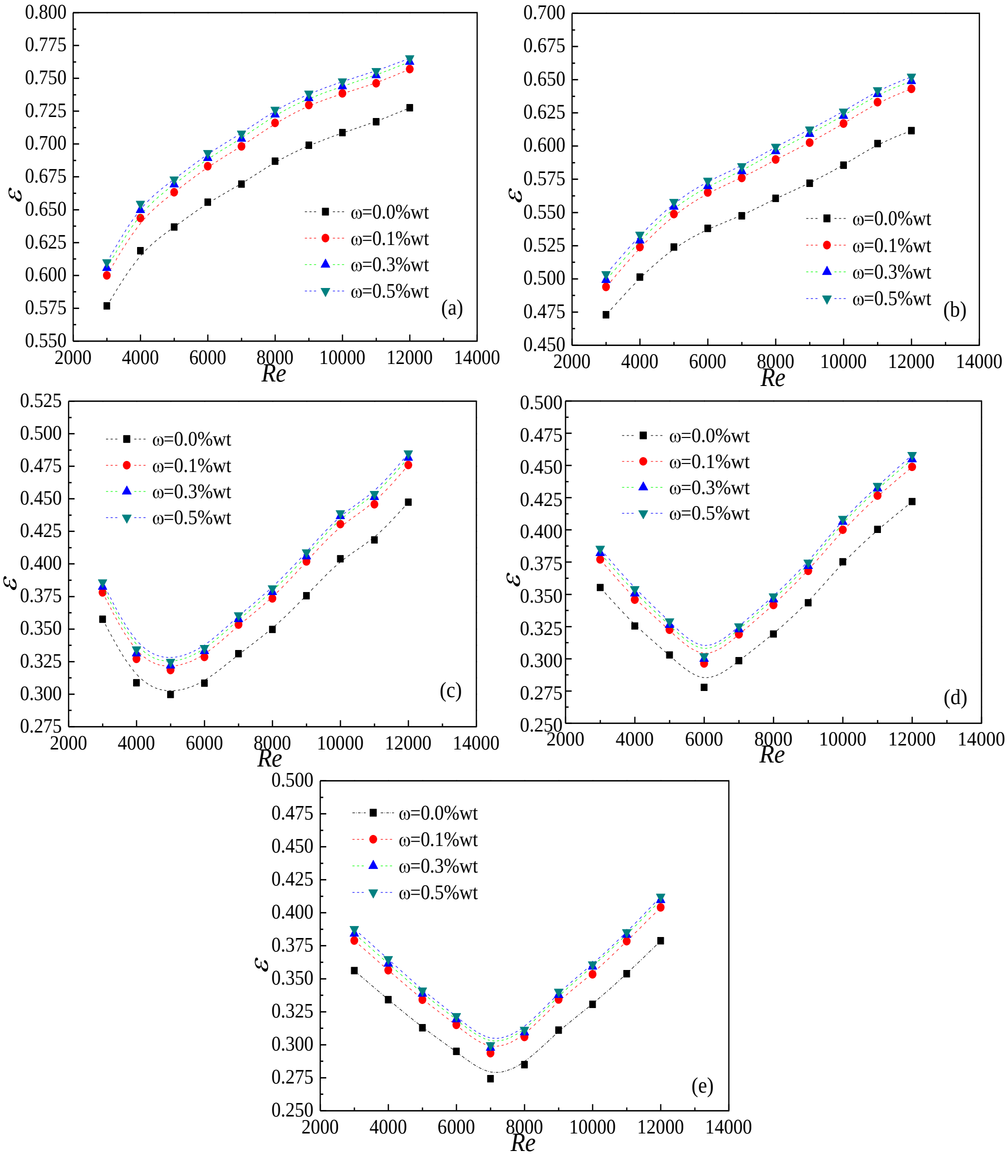

Fig. 11. Effects of nanoparticle mass fraction on the effectiveness of the corrugated double-tube heat exchanger, (a) q_v=1L/min, (b) q_v=2L/min, (c) q_v=3L/min, (d) q_v=4L/min, (e) q_v=5L/min

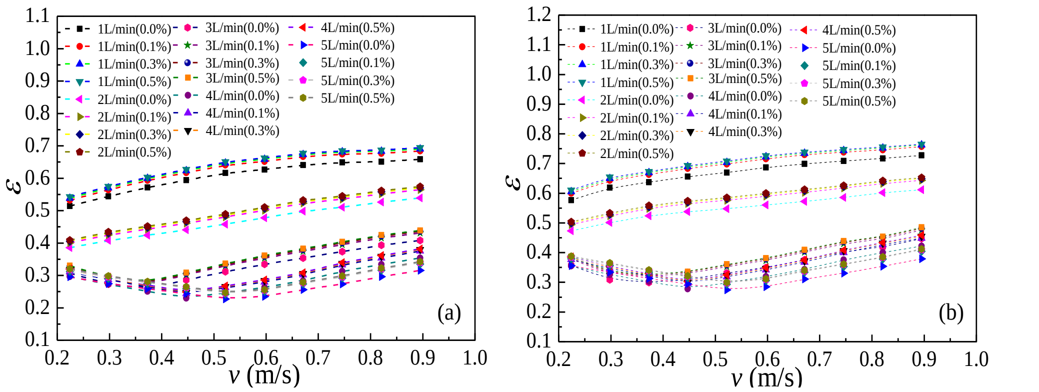

Fig. 12. The summary graph on the effectiveness with velocity, (a) smooth tube, (b) corrugated tube

addition and corrugated tube used in this experiment make the heat transfer capacity significantly higher than the traditional smooth tube and deionized water.

3.3.1.4 Pressure drop

For the practical application of nanofluids, studying the flow and heat transfer performances is inevitable. Adding nanoparticles into base fluid can improve the heat conductivity, but it also increases the flow resistance. This section will discuss the pressure drop of nanofluids in tube-side.

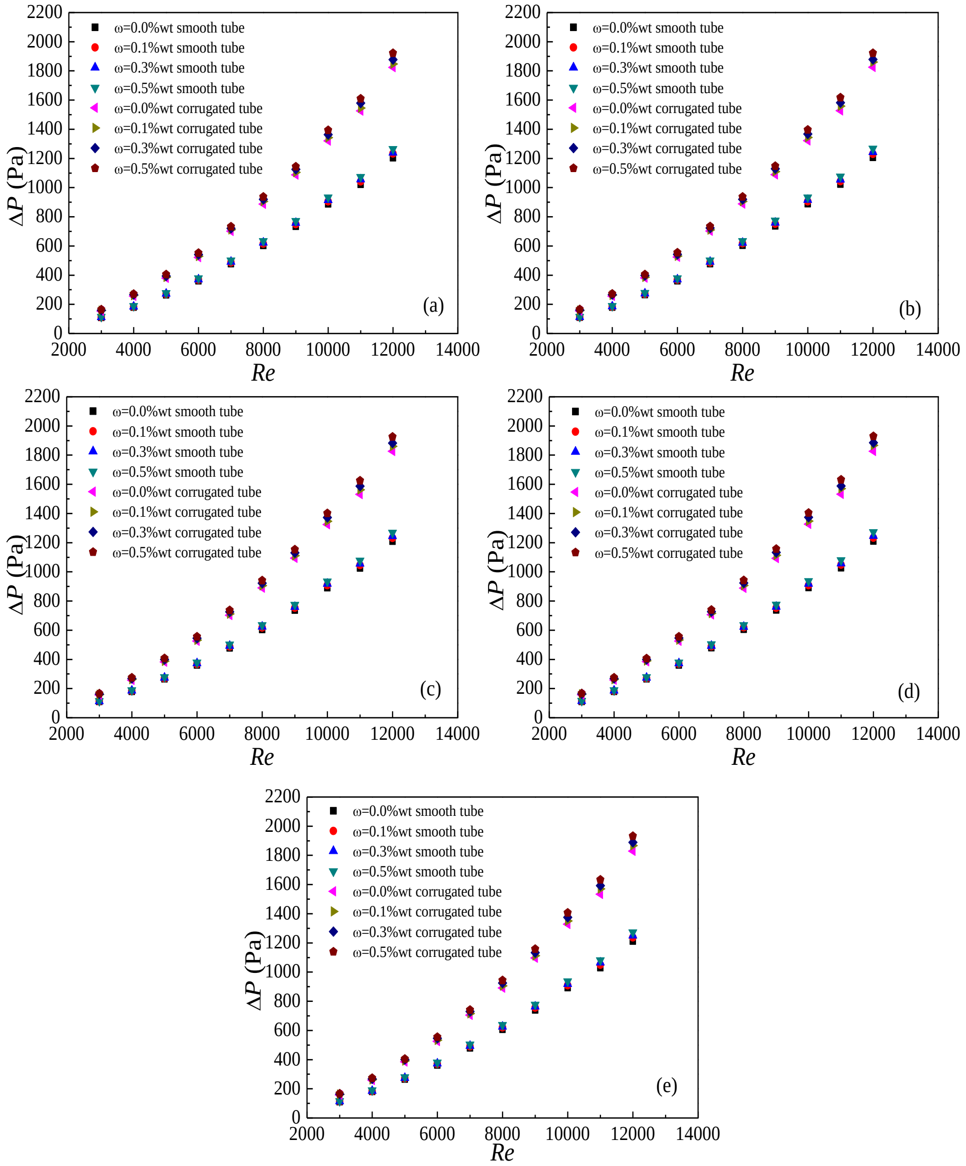

Fig. 13. Effects of nanoparticle mass fraction on the pressure drop of the two kinds of double-tube heat exchangers, (a) q_v=1L/min, (b) q_v=2L/min, (c) q_v=3L/min, (d) q_v=4L/min, (e) q_v=5L/min

The results also show the pressure drop augment with the increase of nanofluids concentrations, which can be explained by that the addition of the nanoparticles increases the friction-induced property, namely, dynamic viscosity. Compared with deionized water, the pressure drop of nanofluids with ω=0.1%, 0.3% and 0.5% is improved by 2.77%, 4.38% and 6.5% at best respectively in the corrugated double-tube heat exchanger. Furthermore, Fig. 13 also shows that the different thermal fluid flow rates in shell-side hardly have effect on the pressure drop of nanofluids, which is because the thermal fluid belongs to the shell-side circuit, and the fluid flow states of thermal fluid and nanofluids do not affect each other.

When comparing the pressure drop of two kinds of double-tube heat exchangers, Fig. 13 shows that the pressure drop in the corrugated tube is significantly stronger, and under the same conditions, it can be increased by 51.9% at best compared with that of the smooth tube.

3.3.1.5 Comprehensive performance analysis

There are many indexes for evaluating the comprehensive performance of heat exchanger, and *PEC* evaluation method is widely used, but it is troublesome to calculate the Nusselt number of the all experimental conditions. Therefore, *EEC* (efficiency evaluation criterion) is obtained as the comprehensive evaluation criteria in this experiment, and the calculation equation is as follows [89]:

$$EEC = \frac{Q / Q_0}{(V\Delta P) / (V_0 \Delta P_0)} \tag{12}$$

In the formula, Q represents the amount of heat exchange rate, and V represents the volume flow rate. The Q/Q_0 and the $(V\Delta P)/(V_0\Delta P_0)$ represent the ratio of thermal transfer and the pump power consumption between the enhanced tube and the smooth tube respectively. Therefore, the *EEC* is also a comprehensive indicator of heat exchangers (thermal efficiency).

Deionized water with the smallest mass flow rate (q_v=1L/min) shows the lowest thermal performance, in order to investigate the largest heat transfer enhancement ratio, other working conditions are all compared with deionized water with q_v=1L/min. According to the *EEC* formula, this experiment compares of nanofluids (all the experimental conditions) and deionized water (q_v=1L/min) in the smooth double-tube heat exchanger. The comparison results are shown in Fig. 14(a). At the same time, all the experimental conditions in the corrugated double-tube heat exchanger are also compared with deionized water (q_v=1L/min) in the smooth double-tube heat exchanger. The comparison results are shown in Fig. 14(b).

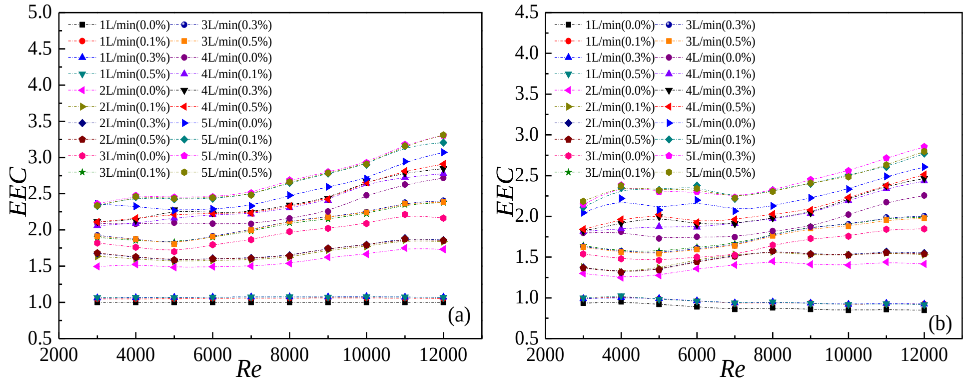

Fig. 14. Comprehensive performance analysis of the tube-side nanofluids, (a) smooth tube, (b) corrugated tube

Fig. 14 manifests that the maximum comprehensive evaluation coefficients in the smooth double-tube heat exchanger are 1.78, 1.885, 2.4, 2.91 and 3.31 respectively when the volume flow rates of thermal fluid are from 1L/min to 5L/min. And the maximum comprehensive evaluation coefficients in the corrugated double-tube heat exchanger are 1.025, 1.576, 2.01, 2.51 and 2.85 respectively when the thermal fluid flow rates are from 1L/min to 5L/min. Through comparing the maximum comprehensive evaluation coefficient of the smooth and corrugated heat exchangers, it is indicated that the maximum comprehensive evaluation coefficient is lower in the corrugated double-tube heat exchanger under the same conditions. The reason is that in the condition of thermal fluid in shell-side and nanofluids in tube-side, although the corrugated tube can disturb the fluid to improve the heat exchange capacity, the pressure drop significantly increases, hence, the comprehensive performance index of the corrugated double-tube heat exchanger is lower. Therefore, this layout (thermal fluid in shell-side and nanofluids in tube-side) is not the best choice to obtain the best comprehensive performance of the combination of corrugated tube and nanofluids.

3.3.2 Shell side-nanofluids and tube side-water

The smooth and corrugated double-tube heat exchangers (nanofluids in shell-side and thermal fluid (deionized-water) in tube-side) are experimentally studied in this section respectively. The working fluids in shell-side are TiO_2-H_2O nanofluids with different mass fractions (ω=0.0wt%, 0.1wt%, 0.3wt% and 0.5wt%), the inlet temperature is 20°C, and the Reynolds numbers range from 3000 to 12000. The working fluid in tube-side is thermal fluid (deionized water) with different volume flow rates (q_v=1-5L/min), and the inlet temperature is 40°C.

3.3.2.1 Heat transfer rate

Fig. 15 and Fig. 16 show the effects of nanoparticle mass fractions and different volume flow rates of thermal fluid in tube-side on the heat transfer rate in two kinds of double-tube heat exchanger, and Fig. 17 is a summary graph on heat transfer rate with velocity. Results show that when the thermal fluid flow rate is constant, the heat transfer rate is improved with the Reynolds number, which is due to the increasing turbulence. Furthermore, with the increase of nanofluids concentrations, the heat transfer rate increases, and it can be also improved by the increase of the thermal fluid flow rate, and these experimental phenomena are basically consistent with the experimental conclusions in the previous experiment. However, compared with the previous experiment, the heat transfer rate (nanofluids in shell-side and thermal fluid in tube-side) is stronger that of (nanofluids in tube-side and thermal fluid in

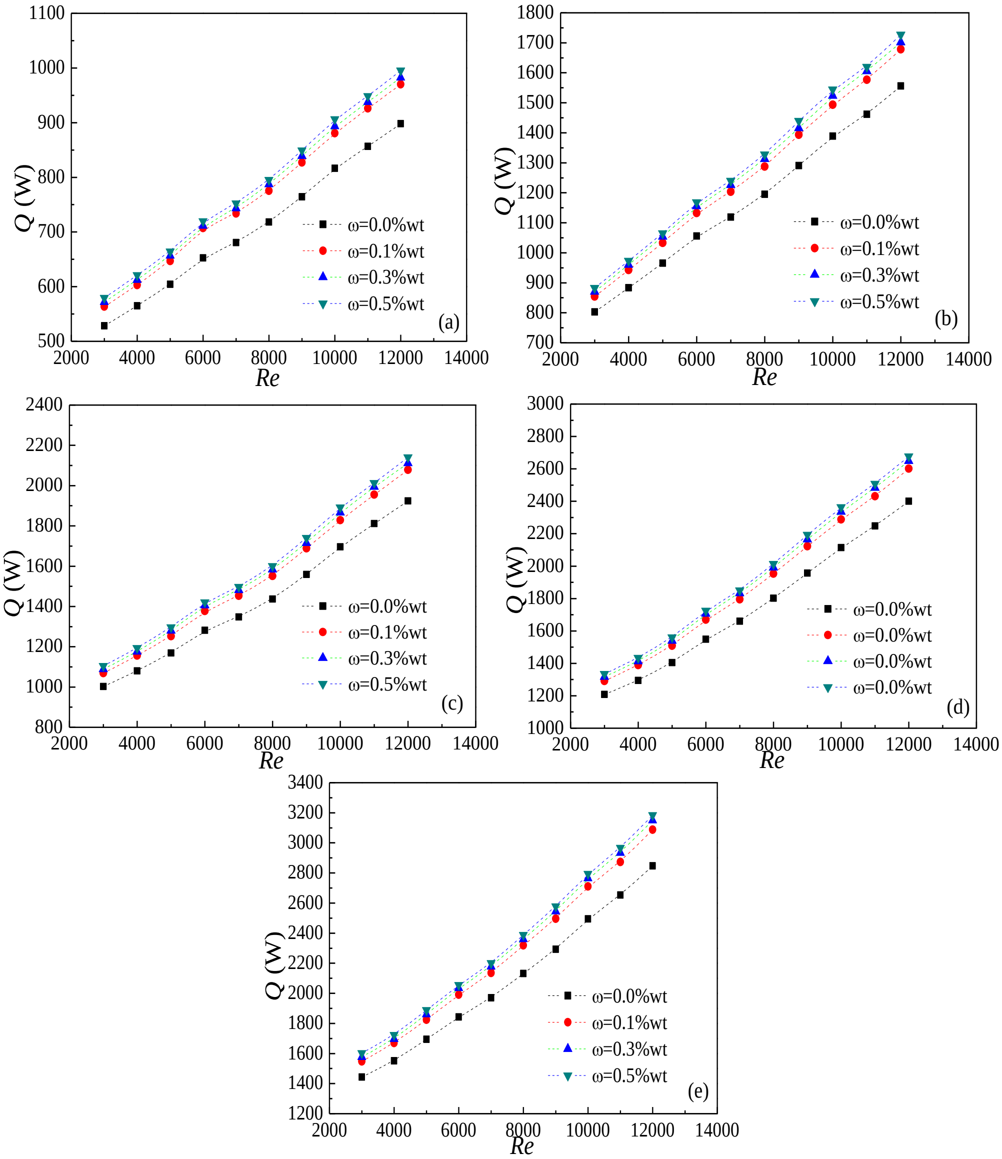

Fig. 15. Effects of nanoparticle mass fraction on the heat transfer rate of the smooth double-tube heat exchanger, (a) q_v=1L/min, (b) q_v=2L/min, (c) q_v=3L/min, (d) q_v=4L/min, (e) q_v=5L/min

shell-side), which is mainly because when the nanofluids flow in the shell-side, the same Reynolds number of nanofluids will cause a larger volume flow rate, which leads to the improvement of the heat transfer rate.

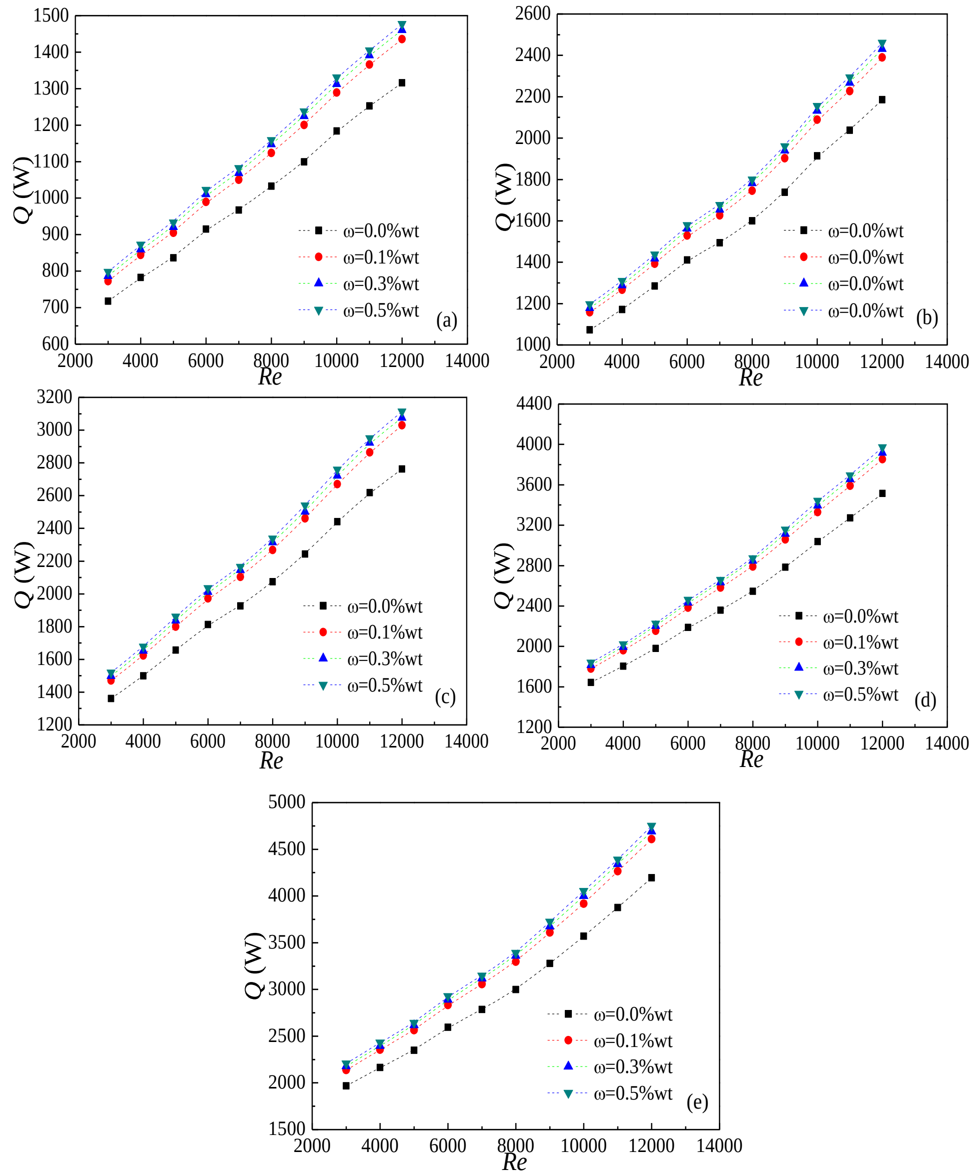

Fig. 16. Effects of nanoparticle mass fraction on the heat transfer rate of the corrugated double-tube heat exchanger, (a) q_v=1L/min, (b) q_v=2L/min, (c) q_v=3L/min, (d) q_v=4L/min, (e) q_v=5L/min

As displayed in Figs. 15-17, the heat transfer rate of the corrugated double-tube heat exchanger is stronger, and it can be improved by 49.2% at best compared with smooth inner tube under the same condition. Furthermore, it can be also improved by

10.08%, 12.1% and 13.6% at best using nanofluids with ω=0.1wt%, 0.3wt% and 0.5wt% compared with deionized water respectively. Compared the maximum thermal enhancement of nanofluids with the previous experiment, it is indicated that nanofluids with ω=0.1%, 0.3% and 0.5% in this experiment have lower heat transfer enhancement. This is mainly because the corrugated tube used in the experiment has a greater disturbance in the tube-side than that in the shell-side, furthermore, the larger flow rate also causes the collision and friction frequency between the solid nanoparticles and the heat transfer surface to be weak when nanofluids flow in the shell-side.

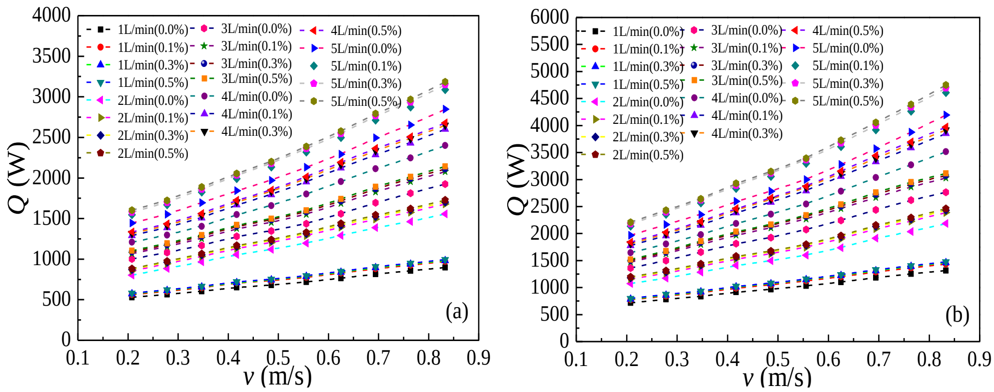

Fig. 17. The summary graph on the heat transfer rate with velocity, (a) smooth tube, (b) corrugated tube

3.3.2.2 *NTU*

In a heat exchanger, the *NTU* and effectiveness are two important indicators for evaluating the overall thermal performance. The *NTU* results of smooth and corrugated double-tube heat exchangers are demonstrated in Fig. 18 and Fig. 19 respectively. The summary graph on the *NTU* with velocity is shown in Fig. 20.

The *NTU* trends of this experiment don't show a tendency to increase firstly and then decrease. This can be explained that the flow rate of nanofluids in the shell-side is larger than that in the tube-side under the same Reynolds number, the *NTU* is determined from the overall heat exchanger, which varies with the flow rates in shell-side and tube-side.

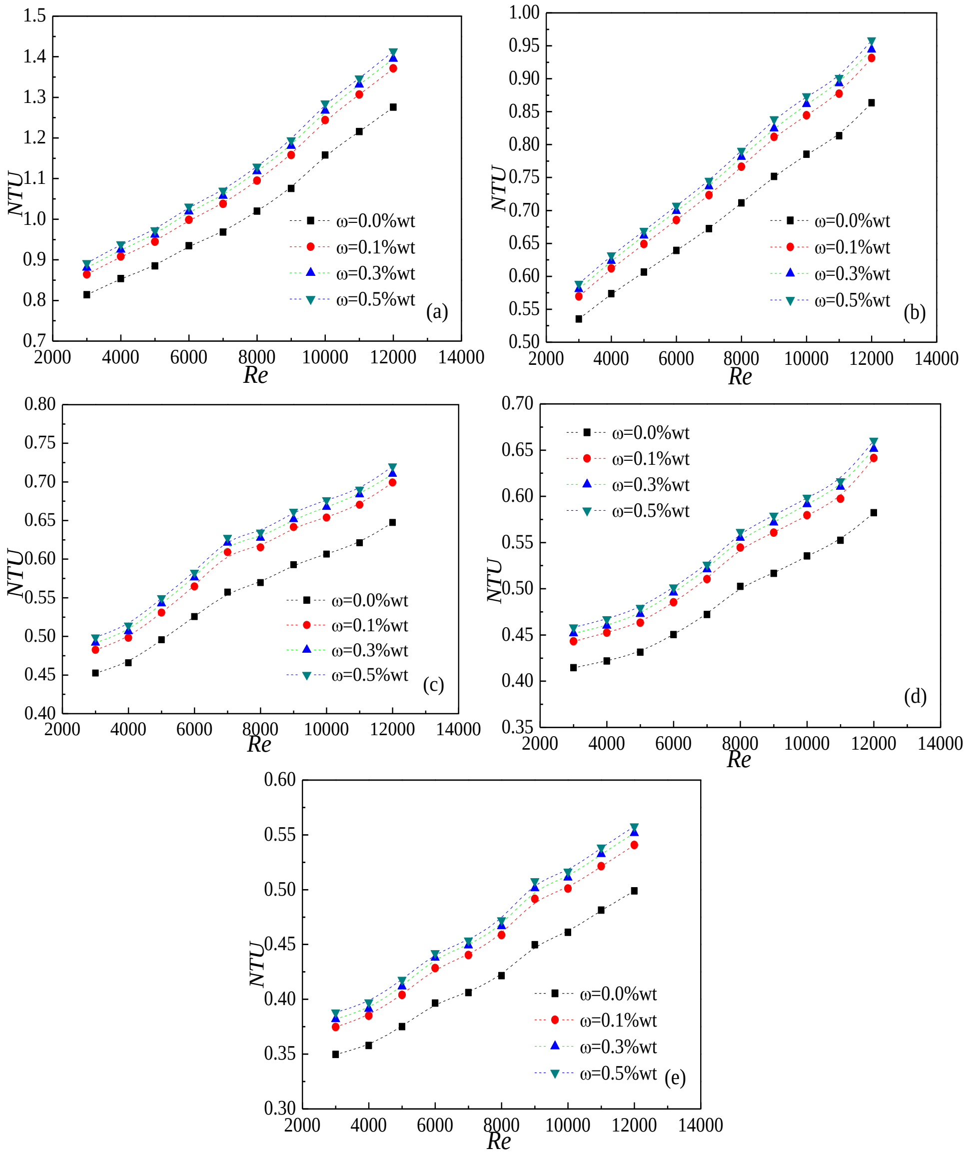

Fig. 18. Effects of nanoparticle mass fraction on *NTU* of the smooth double-tube heat exchanger, (a) q_v=1L/min, (b) q_v=2L/min, (c) q_v=3L/min, (d) q_v=4L/min, (e) q_v=5L/min

Figs. 18-20 also show that when the thermal fluid volume flow rate is constant, as the Reynolds number in shell-side increases, the *NTU* also increases correspondingly. Increasing Reynolds number in shell-side can significantly improve the thermal performance at this time. Furthermore, under the same thermal fluid flow rate, the *NTU* can be improved by 42.8% at best in the corrugated double-tube heat exchanger.

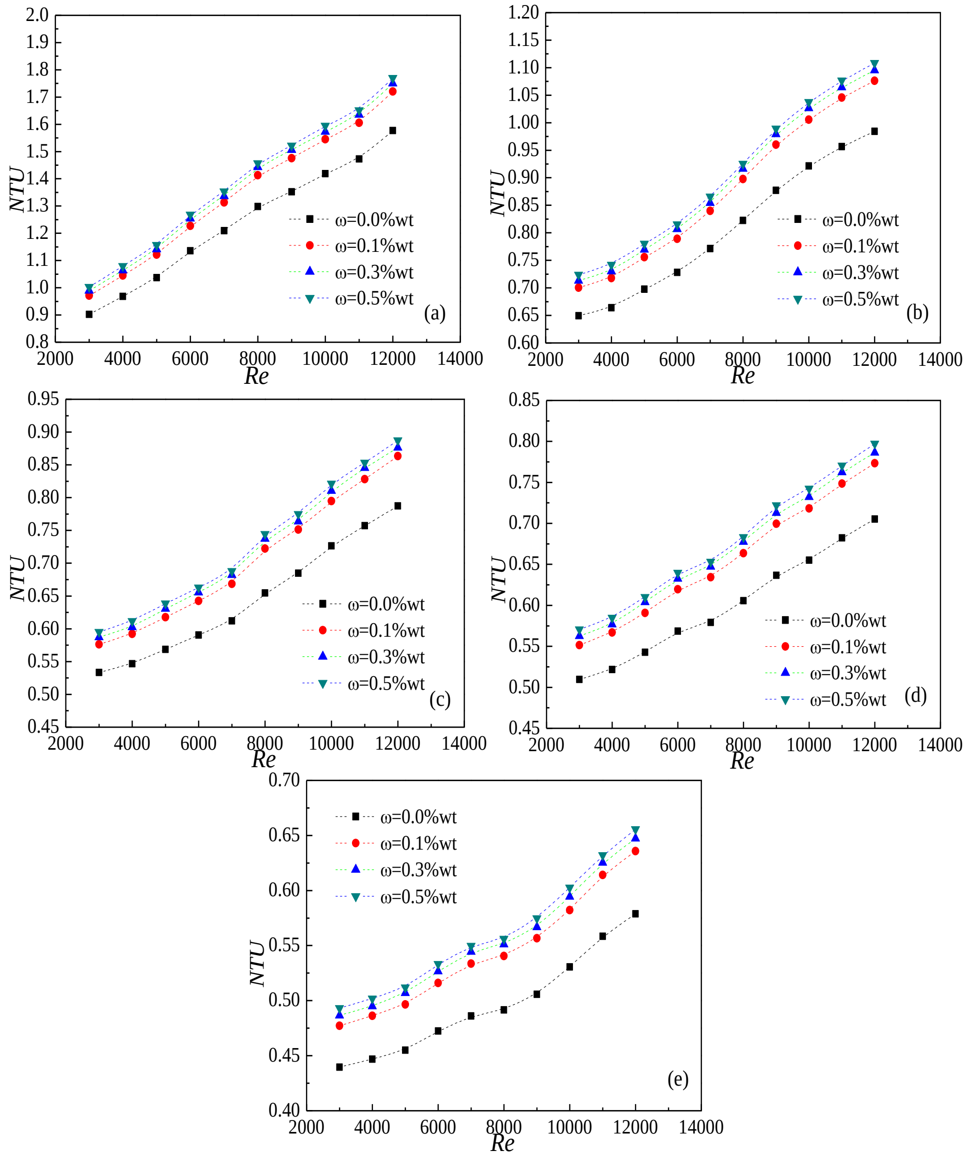

Fig. 19. Effects of nanoparticle mass fraction on *NTU* of the corrugated double-tube heat exchanger, (a) q_v=1L/min, (b) q_v=2L/min, (c) q_v=3L/min, (d) q_v=4L/min, (e) q_v=5L/min

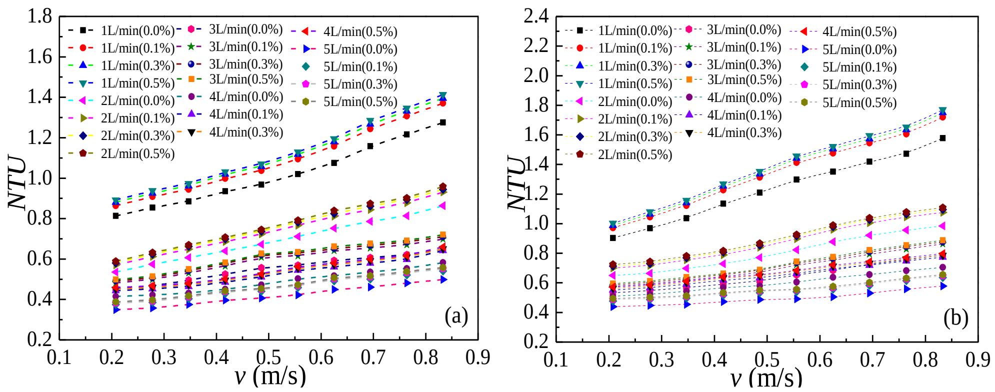

Fig. 20. The summary graph on the *NTU* with velocity, (a) smooth tube, (b) corrugated tube

3.3.2.3 Effectiveness

The variations of effectiveness against Reynolds number in shell-side are depicted in Fig. 21 and Fig. 22, and the summary graph on the effectiveness with velocity is shown in Fig. 23. The influence of different nanoparticle mass fractions and thermal fluid flow rates on the effectiveness is discussed. With the increase of the nanofluids concentration and Reynolds number, the effectiveness increases correspondingly. And the effectiveness is stronger in the corrugated double-tube heat

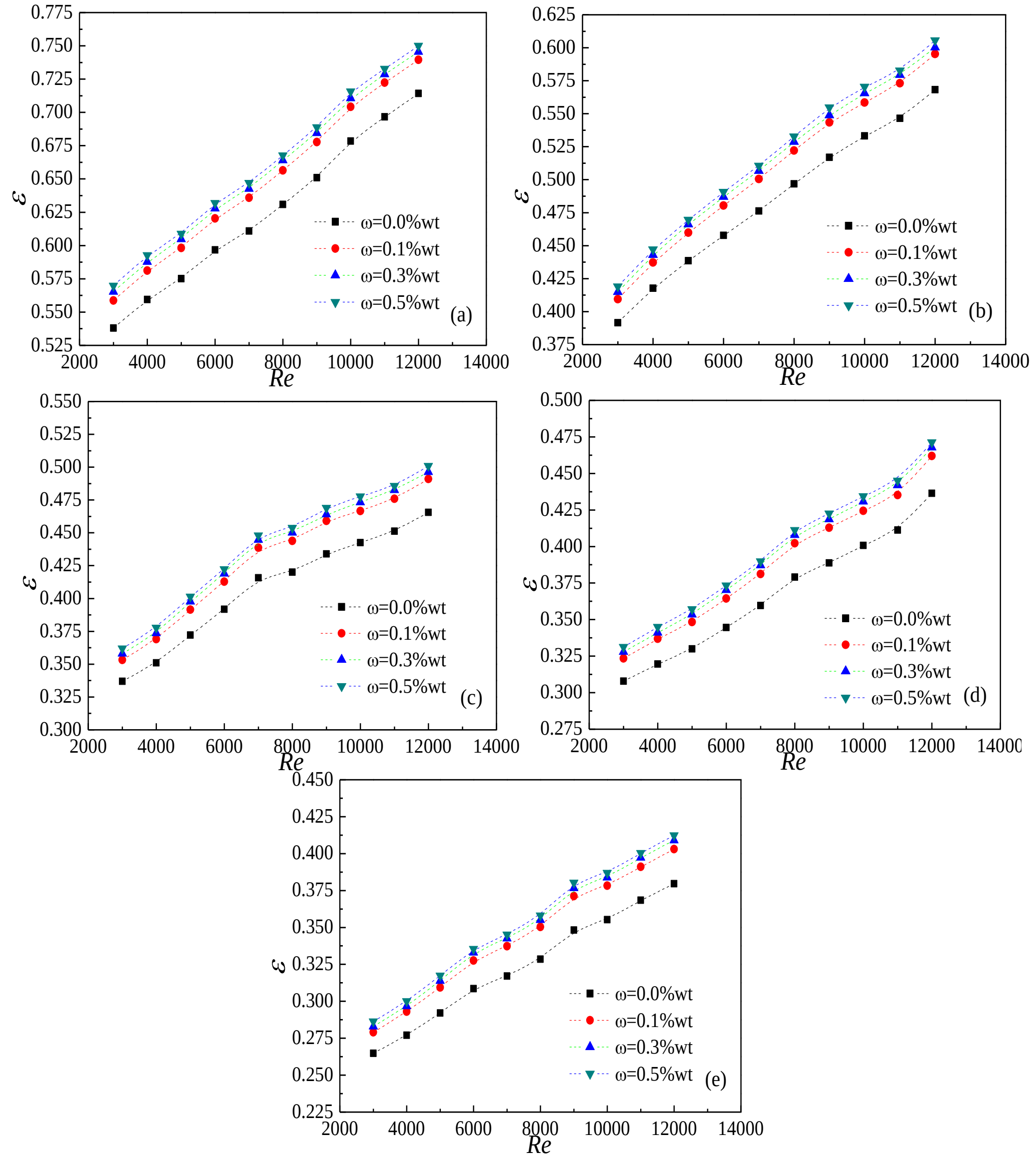

Fig. 21. Effects of nanoparticle mass fraction on the effectiveness of the smooth double-tube heat exchanger, (a) q_v=1L/min, (b) q_v=2L/min, (c) q_v=3L/min, (d) q_v=4L/min, (e) q_v=5L/min

exchanger under the same condition.

In order to intuitively express the influence of the nanofluids concentration on the effectiveness, this experiment takes the flow rate in tube-side q_v=5L/min and Reynolds number in shell-side Re=9000 as an example for comparative analysis. When the working medium in shell-side is deionized water, the effectiveness of the corrugated double-tube heat exchanger is 37.9%, and the effectiveness of nanofluids with ω=0.1wt%, 0.3wt% and 0.5wt% can reach 40.6%, 41.2% and 41.6%

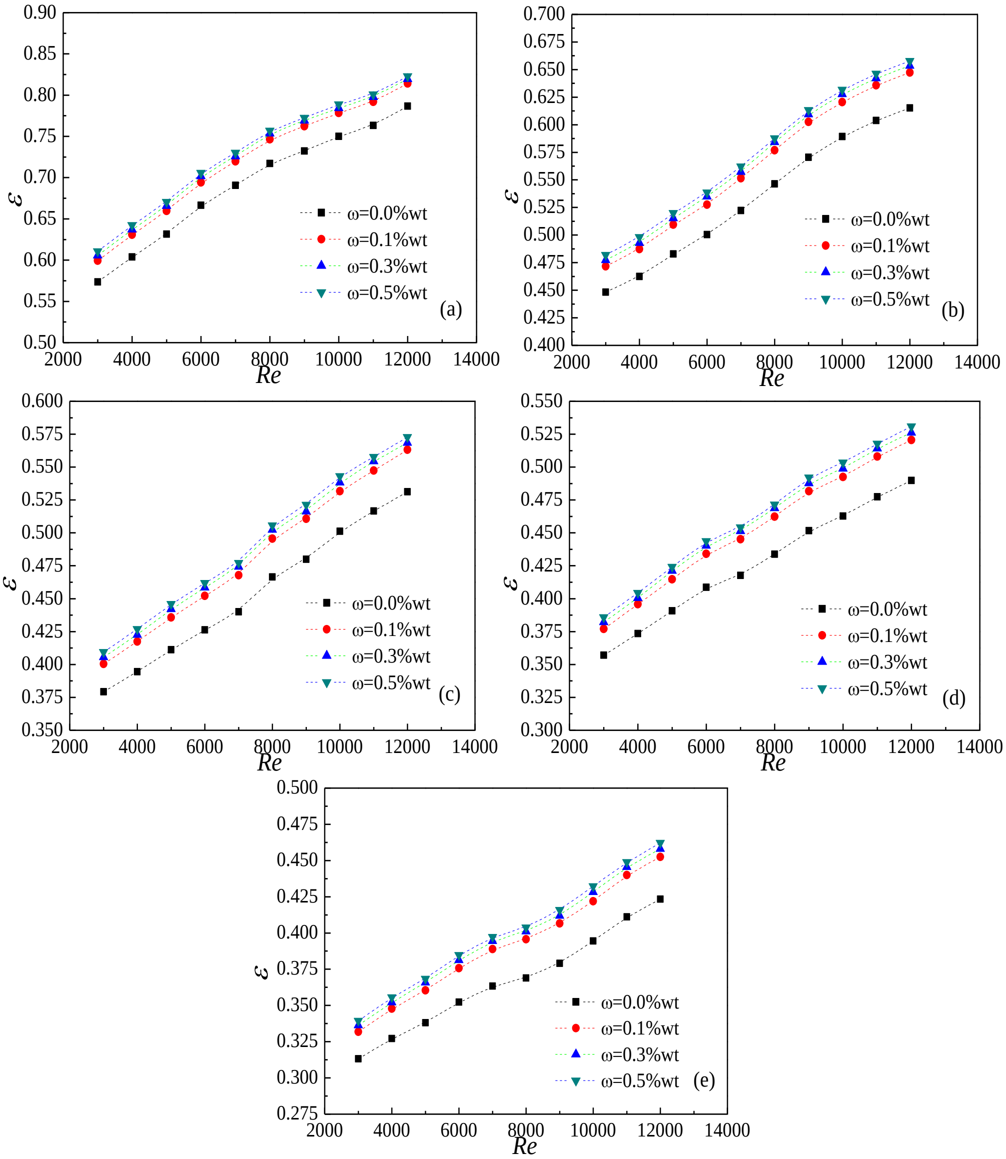

Fig. 22. Effects of nanoparticle mass fraction on the effectiveness of the corrugated double-tube heat exchanger, (a) q_v=1L/min, (b) q_v=2L/min, (c) q_v=3L/min, (d) q_v=4L/min, (e) q_v=5L/min

respectively.

Furthermore, intuitive comparative analysis of the effectiveness of two kinds of double-tube heat exchangers can be also obtained from Figs. 21-23. This experiment takes the volume flow rates in tube-side (from 1L/min to 5L/min) and the Reynolds number in shell-side *Re*=9000 as an example, for the combination of deionized water and smooth double-tube heat exchanger, the effectiveness can reach 65.1%, 51.7%, 43.4%, 38.8% and 34.8% under different volume flow rates respectively. For the combination of nanofluids and corrugated double-tube heat exchanger, the effectiveness can reach 77.2%, 61.3%, 52.1%, 49.2% and 41.6% under different thermal fluid flow rates respectively. From the comparison, it can be found that although the effectiveness decreases with the thermal fluid flow rate, the combination of the corrugated tube and nanofluids can obviously improve the effectiveness of the double-tube heat exchangers.

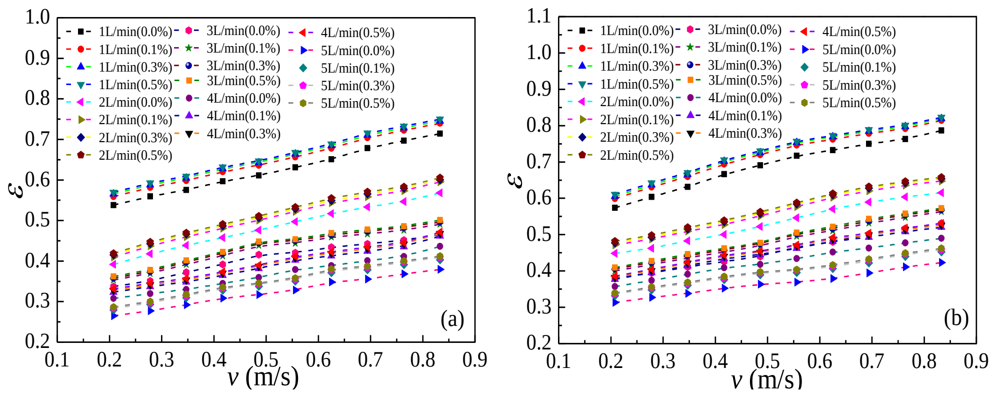

Fig. 23. The summary graph on the effectiveness with velocity, (a) smooth tube, (b) corrugated tube

3.3.2.4 Pressure drop

In the experiment of this section, the shell-side working fluid is nanofluids. Therefore, in the smooth and corrugated double-tube heat exchangers, this experiment mainly studies the variation of the shell-side pressure drop. Fig. 24 presents the effects of nanofluids concentration and thermal fluid flow rate on the pressure drop of smooth and corrugated double-tube heat exchangers. Fig. 24 manifests that there is almost no difference in the pressure drop of nanofluids when the thermal fluid volume flow rate changes, which is mainly because that the thermal fluid and nanofluids are two independent loops, and the flow states between the two fluids do not interfere with each other.

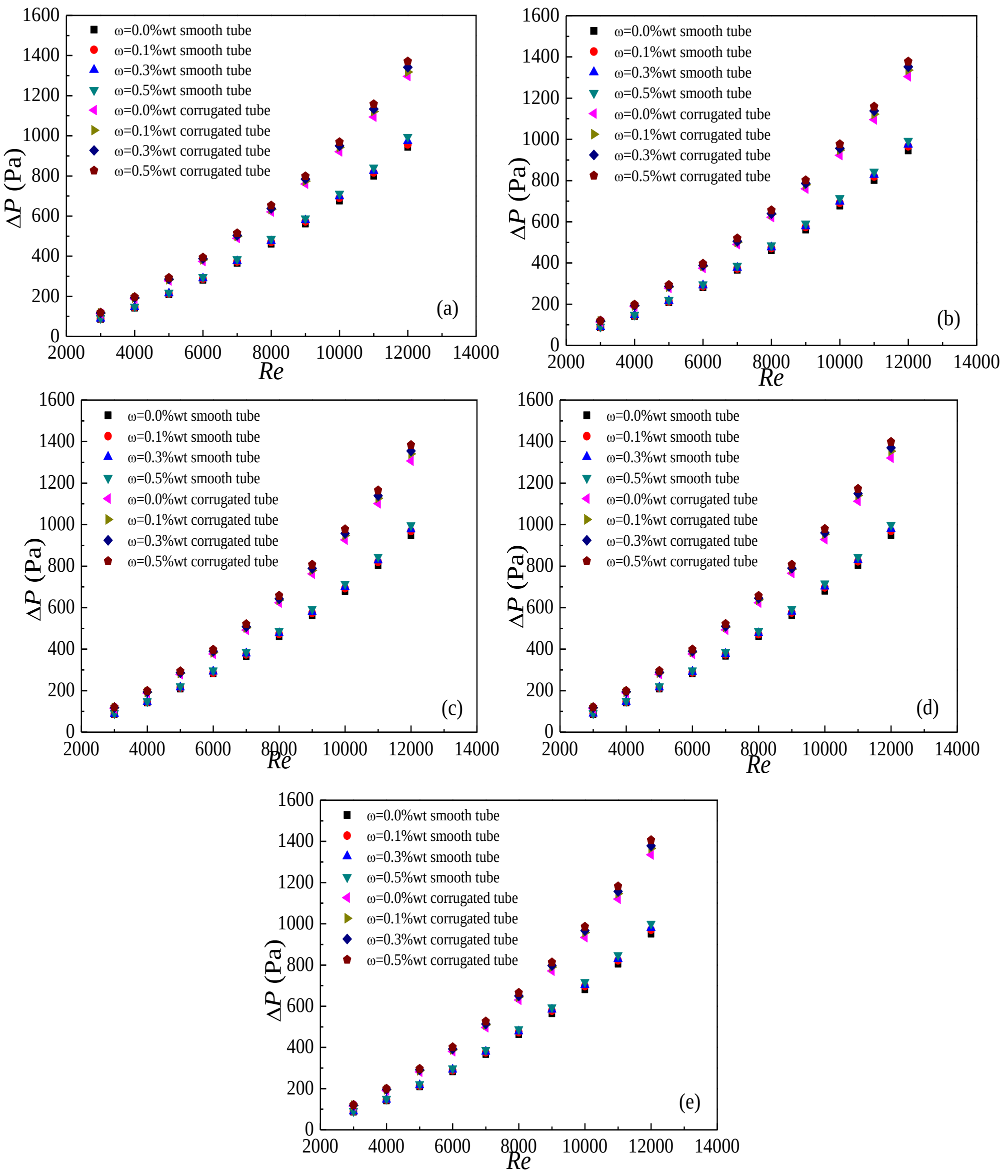

Fig. 24. Effects of nanoparticle mass fraction on the drop pressure in shell-side of the smooth and corrugated double-tube heat exchangers, (a) q_v=1L/min, (b) q_v=2L/min, (c) q_v=3L/min, (d) q_v=4L/min, (e) q_v=5L/min

Through the comparison between the pressure drop of the two kinds of double-tube heat exchanger, it is indicated that the pressure drop in the corrugated double-tube heat exchanger is significantly stronger, and the maximum increase in pressure drop can reach 40.7% under the same thermal fluids flow rate, which also shows that the increase is smaller than that of the previous experiment.

Furthermore, the viscosity of the nanofluids is higher than that of the deionized water, so that the nanofluids have a greater flow resistance than the deionized water. In the corrugated double-tube heat exchanger, the pressure drop of nanofluids with ω=0.1wt%, 0.3wt% and 0.5wt% is improved by 2.77%, 3.89% and 5.97% at best compared with deionized water respectively. Therefore, the influence of the nanoparticle concentration on the pressure drop is smaller than the disturbance of the corrugated tube.

3.3.2.5 Comprehensive performance analysis

The *EEC* formula in this section considers the heat transfer rate and the shell-side pressure drop. Fig. 25(a) compares all experimental conditions of nanofluids (ω=0.0wt%, 0.1wt%, 0.3wt% and 0.5wt%) in the smooth double-tube heat exchanger with deionized water (q_v=1L/min) in the smooth double-tube heat exchanger. Fig. 25(b) provides a comprehensive comparison between all experimental conditions of nanofluids (ω=0.0wt%, 0.1wt%, 0.3wt% and 0.5wt%) in the corrugated double-tube heat exchanger and deionized water (q_v=1L/min) in the smooth double-tube heat exchanger. Fig. 25(a) presents that when the thermal fluid flow rates are from 1L/min to 5L/min, the maximum *EEC* values are 1.06, 1.79, 2.27, 2.84 and 3.37 respectively. In Fig. 25(b), the maximum *EEC* values are 1.15, 1.88, 2.38, 3.01

and 3.56 respectively. It can be intuitively seen from the *EEC* that when the flow pattern of the thermal fluid in tube-side and nanofluids in shell-side is selected, the maximum comprehensive performance index of nanofluids and corrugated tube combination is stronger than that of nanofluids and smooth tube combination under the same thermal fluid flow rate. Therefore, the selection of the nanofluids flowing in the shell-side can not only reflect the heat transfer enhancement of the nanofluids, but also reflect the thermal performance of the corrugated tube.

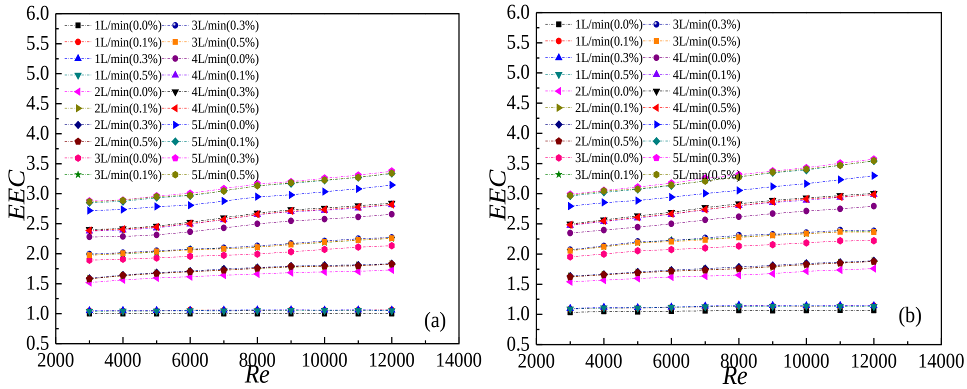

Fig. 25. Comprehensive performance analysis of nanofluids in the shell-side, (a) smooth tube, (b) corrugated tube

The comparative analysis of this experiment and the previous experiment are studied. In the previous experiment, it has been concluded that when the nanofluids flow in the tube-side, the pressure drop of nanofluids can be improved by 51.9% at best. However, when the nanofluids flow in the shell-side, the pressure drop can be improved by 40.7% at best. Furthermore, nanofluids flow in the shell-side can also have a greater heat transfer rate, which is mainly due to the less contact with the external environment, and when the Reynolds number of the nanofluids is kept constant, nanofluids flowing in the shell-side will have a larger flow rate, then the heat transfer rate becomes larger. Therefore, regardless of the actual application, or the comparison of comprehensive performance, the choice of thermal fluid in the tube-side and nanofluids in the shell-side will be more appropriate.

4 Conclusion

The thermal performance and pressure drop of nanofluids in the smooth and corrugated double-tube heat exchangers are experimentally investigated, and the experimental results are compared between these two kinds of double-tube heat exchangers. Some main conclusions are obtained as follows:

(1) TiO_2-H_2O nanofluids with ω=0.1wt%, 0.3wt% and 0.5wt% have better thermal performance than the deionized water, the heat transfer rate can be improved by 10.8%, 13.4% and 14.8% at best respectively, and the pressure drop of nanofluids can be increased by 2.77%, 4.38% and 6.5% at best respectively.

(2) The thermal performance of the corrugated double-tube heat exchanger is significantly stronger than that of the same size smooth double-tube heat exchanger. But the pressure drop of nanofluids in the corrugated double-tube heat exchanger is also significantly stronger, and it can be increased by 51.9% (tube-side) and 40.7% (shell-side) at best.

(3) When using both nanofluids and corrugated tube, the overall thermal performance is significantly enhanced, which reflects in the increase of the *NTU* and effectiveness. *NTU* can be improved by 47.5% at best. However, for thermal fluid in the shell-side, the *NTU* and effectiveness decrease firstly and then increase with the increase of Reynolds number.

(4) When nanofluids flow in the tube-side, the comprehensive performance index of the corrugated tube is lower than that of the smooth tube under the same

conditions.

(5) When nanofluids flow in the shell-side, the comprehensive performance index is stronger than that of the smooth tube under the same condition. Therefore, in practical applications, it is more reasonable to select the flow mode of thermal fluid in the tube-side and nanofluids in the shell-side.

Acknowledgements

This work is financially supported by "National Natural Science Foundation of China" (Grant No. 51606214), "Natural Science Foundation of Jiangsu Province, China" (Grant No. BK20181359) and "EU ThermaSMART project, H2020-MSCA-RISE (778104)-Smart thermal management of high power microprocessors using phase-change (ThermaSMART)".

References

[1] Sajid MU, Ali HM. Thermal conductivity of hybrid nanofluids: A critical review. Int J Heat Mass Transf 2018; 126: 211-234.

[2] Ranjbarzadeh R, Moradikazerouni A, Bakhtiari R, Asadi A, Afrand M. An experimental study on stability and thermal conductivity of water/silica nanofluid: Eco-friendly production of nanoparticles. J Clean Prod 2019; 206: 1089-1100.

[3] Asadi A, Pourfattah F. Heat transfer performance of two oil-based nanofluids containing ZnO and MgO nanoparticles; a comparative experimental investigation. Powder Technol 2019; 343: 296-308.

[4] Esfahani NN, Toghraie D, Afrand M. A new correlation for predicting the thermal conductivity of ZnO-Ag (50%–50%)/water hybrid nanofluid: An experimental

study. Powder Technol 2018; 323: 367-373.

[5] Esfe MH, Esfandeh S, Afrand M, Rejvani M, Rostamian SH. Experimental evaluation, new correlation proposing and ANN modeling of thermal properties of EG based hybrid nanofluid containing ZnO-DWCNT nanoparticles for internal combustion engines applications. Appl Therm Eng 2018; 133: 452-463.

[6] Safaei MR, Hajizadeh A, Afrand M, Qi C, Yarmand H, Zulkifli NWBM. Evaluating the effect of temperature and concentration on the thermal conductivity of ZnO-TiO_2/EG hybrid nanofluid using artificial neural network and curve fitting on experimental data. Physica A 2019; 519: 209-216.

[7] Asadi A, Asadi M, Rezaniakolaei A, Rosendahl LA, Wongwises S. An experimental and theoretical investigation on heat transfer capability of Mg $(OH)_2$/MWCNT-engine oil hybrid nano-lubricant adopted as a coolant and lubricant fluid. Appl Therm Eng 2018; 129: 577-586.

[8] Asadi A, Aberoumand S, Moradikazerouni A, Pourfattah F, Żyła G, Estelle P, Mahian O, Wongwises S, Nguyen HM, Arabkoohsar A. Recent advances in preparation methods and thermophysical properties of oil-based nanofluids: A state-of-the-art review. Powder Technol 2019; 352: 209-226.

[9] Asadi A. A guideline towards easing the decision-making process in selecting an effective nanofluid as a heat transfer fluid. Energy Convers Manage 2018; 175: 1-10.

[10] Zeng J, Xuan Y. Tunable full-spectrum photo-thermal conversion features of magnetic-plasmonic Fe_3O_4/TiN nanofluid. Nano Energy 2018; 51: 754-763.

[11] Liu X, Xuan Y. Full-spectrum volumetric solar thermal conversion via photonic nanofluids. Nanoscale 2017; 9(39): 14854-14860.

[12] Li H, He Y, Wang C, Wang X, Hu Y. Tunable thermal and electricity generation enabled by spectrally selective absorption nanoparticles for photovoltaic/thermal applications. Appl Energy 2019; 236: 117-126.

[13] Shi L, He Y, Wang X, Hu Y. Recyclable photo-thermal conversion and purification systems via Fe_3O_4@TiO_2 nanoparticles. Energy Convers Manage 2018; 171: 272-278.

[14] Shi L, He Y, Huang Y, Jiang B. Recyclable Fe_3O_4@CNT nanoparticles for high-efficiency solar vapor generation. Energy Convers Manage 2017; 149: 401-408.

[15] Wang X, He Y, Cheng G, Shi L, Liu X, Zhu J. Direct vapor generation through localized solar heating via carbon-nanotube nanofluid. Energy Convers Manage 2016; 130: 176-183.

[16] Liu X, Wang X, Huang J, Cheng G, He Y. Volumetric solar steam generation enhanced by reduced graphene oxide nanofluid. Appl Energy 2018; 220: 302-312.

[17] Wang X, He Y, Liu X. Synchronous steam generation and photodegradation for clean water generation based on localized solar energy harvesting. Energy Convers Manage 2018; 173: 158-166.

[18] Fan LW, Li JQ, Wu YZ, Zhang L, Yu ZT. Pool boiling heat transfer during quenching in carbon nanotube (CNT)-based aqueous nanofluids: Effects of length

and diameter of the CNTs. Appl Therm Eng 2017; 122: 555-565.

[19] Fan LW, Yao XL, Wang X, Wu YY, Liu XL, Xu X, Yu ZT. Non-isothermal crystallization of aqueous nanofluids with high aspect-ratio carbon nano-additives for cold thermal energy storage. Appl Energy 2015; 138: 193-201.

[20] Asadi A, Asadi M, Rezaniakolaei A, Rosendahl LA, Afrand M, Wongwises S. Heat transfer efficiency of Al_2O_3-MWCNT/thermal oil hybrid nanofluid as a cooling fluid in thermal and energy management applications: An experimental and theoretical investigation. Int J Heat Mass Transf 2018 117: 474-486.

[21] Zhao N, Guo L, Qi C, Chen T, Cui X. Experimental study on thermo-hydraulic performance of nanofluids in CPU heat sink with rectangular grooves and cylindrical bugles based on exergy efficiency. Energy Convers Manage 2019; 181: 235-246.

[22] Zhao N, Qi C, Chen T, Tang J, Cui X. Experimental study on influences of cylindrical grooves on thermal efficiency, exergy efficiency and entropy generation of CPU cooled by nanofluids. Int J Heat Mass Transf 2019; 135: 16-32.

[23] Qi C, Hu J, Liu M, Guo L, Rao Z. Experimental study on thermo-hydraulic performances of CPU cooled by nanofluids. Energy Convers Manage 2017; 153: 557-565.

[24] Qi C, Zhao N, Cui X, Chen T, Hu J. Effects of half spherical bulges on heat transfer characteristics of CPU cooled by TiO_2-water nanofluids. Int J Heat Mass Transf 2018; 123: 320-330.

[25] Sarafraz MM, Nikkhah V, Nakhjavani M, Arya A. Thermal performance of a heat sink microchannel working with biologically produced silver-water nanofluid: experimental assessment. Exp Therm Fluid Sci 2018; 91: 509-519.

[26] Sajid MU, Ali HM, Sufyan A, Rashid D, Zahid SU, Rehman WU. Experimental investigation of TiO_2-water nanofluid flow and heat transfer inside wavy mini-channel heat sinks. J Therm Anal Calorim 2019; https://doi.org/10.1007/s10973-019-08043-9

[27] Arya A, Sarafraz MM, Shahmiri S, Madani SAH, Nikkhah V, Nakhjavani SM. Thermal performance analysis of a flat heat pipe working with carbon nanotube-water nanofluid for cooling of a high heat flux heater. Heat Mass Transf 2018; 54(4): 985-997.

[28] Sadeghinezhad E, Mehrali M, Rosen MA, Akhiani AR, Latibari ST, Mehrali M, Metselaar HSC. Experimental investigation of the effect of graphene nanofluids on heat pipe thermal performance. Appl Therm Eng 2016; 100: 775-787.

[29] Shi L, He Y, Hu Y, Wang X. Thermophysical properties of Fe_3O_4@CNT nanofluid and controllable heat transfer performance under magnetic field. Energy Convers Manage 2018; 177: 249-257.

[30] Selimefendigil F, Öztop HF. Corrugated conductive partition effects on MHD free convection of CNT-water nanofluid in a cavity. Int J Heat Mass Transf 2019; 129: 265-277.

[31] Selimefendigil F, Öztop HF. Mixed convection of nanofluids in a three dimensional cavity with two adiabatic inner rotating cylinders. Int J Heat Mass

Transf 2018; 117: 331-343.

[32] Sajjadi H, Delouei AA, Izadi M, Mohebbi R. Investigation of MHD natural convection in a porous media by double MRT lattice Boltzmann method utilizing MWCNT-Fe_3O_4/water hybrid nanofluid. Int J Heat Mass Transf 2019; 132: 1087-1104.

[33] Sheremet MA, Pop I, Mahian O. Natural convection in an inclined cavity with time-periodic temperature boundary conditions using nanofluids: application in solar collectors. Int J Heat Mass Transf 2018; 116: 751-761.

[34] Miroshnichenko IV, Sheremet MA, Oztop HF, Abu-Hamdeh N. Natural convection of alumina-water nanofluid in an open cavity having multiple porous layers. Int J Heat Mass Transf 2018; 125: 648-657.

[35] Miroshnichenko IV, Sheremet MA, Oztop HF, Abu-Hamdeh N. Natural convection of Al_2O_3/H_2O nanofluid in an open inclined cavity with a heat-generating element. Int J Heat Mass Transf 2018; 126: 184-191.

[36] Bondarenko DS, Sheremet MA, Oztop HF, Ali ME. Natural convection of Al_2O_3/H_2O nanofluid in a cavity with a heat-generating element. Heatline visualization. Int J Heat Mass Transf 2019; 130: 564-574.

[37] Sheremet MA, Pop I. Effect of local heater size and position on natural convection in a tilted nanofluid porous cavity using LTNE and Buongiorno's models. J Mol Liq 2018; 266: 19-28.

[38] Ma Y, Mohebbi R, Rashidi MM, Yang Z, Sheremet MA. Numerical study of MHD nanofluid natural convection in a baffled U-shaped enclosure. Int J Heat

Mass Transf 2019; 130: 123-134.

[39] Sheikholeslami M, Shehzad SA, Li Z. Water based nanofluid free convection heat transfer in a three dimensional porous cavity with hot sphere obstacle in existence of Lorenz forces. Int J Heat Mass Transf 2018; 125: 375-386.

[40] Sheikholeslami M, Seyednezhad M. Simulation of nanofluid flow and natural convection in a porous media under the influence of electric field using CVFEM. Int J Heat Mass Transf 2018; 120: 772-781.

[41] Sheikholeslami M, Rokni HB. Numerical modeling of nanofluid natural convection in a semi annulus in existence of Lorentz force. Comput Method Appl Mechanics Eng 2017; 317: 419-430.

[42] Xu H, Xing Z. The lattice Boltzmann modeling on the nanofluid natural convective transport in a cavity filled with a porous foam. Int Commun Heat Mass Transf 2017; 89: 73-82.

[43] Xu H, Gong L, Huang S, Xu M. Flow and heat transfer characteristics of nanofluid flowing through metal foams. Int J Heat Mass Transf 2015; 83: 399-407.

[44] Mohebbi R, Rashidi MM, Izadi M, Sidik NAC, Xian HW. Forced convection of nanofluids in an extended surfaces channel using lattice Boltzmann method. Int J Heat Mass Transf 2018; 117: 1291-1303.

[45] Karimi A, Afrand M. Numerical study on thermal performance of an air-cooled heat exchanger: Effects of hybrid nanofluid, pipe arrangement and cross section. Energy Convers Manage 2018; 164: 615-628.

[46] Tirandaz N, Dehghan M, Valipour MS. Heat and fluid flow through a helical annulus enhanced by a porous material: A perturbation study. Appl Therm Eng 2017; 112: 1566-1574.

[47] Mehrali M, Sadeghinezhad E, Rosen MA, Latibari ST, Mehrali M, Metselaar HSC, Kazi SN. Effect of specific surface area on convective heat transfer of graphene nanoplatelet aqueous nanofluids. Exp Therm Fluid Sci 2015; 68: 100-108.

[48] Mehrali M, Sadeghinezhad E, Rosen MA, Akhiani AR, Latibari ST, Mehrali M, Metselaar HSC. Heat transfer and entropy generation for laminar forced convection flow of graphene nanoplatelets nanofluids in a horizontal tube. Int Commun Heat Mass Transf 2015; 66: 23-31.

[49] Mehrali M, Sadeghinezhad E, Rosen MA, Akhiani AR, Latibari ST, Mehrali M, Metselaar HSC. Experimental investigation of thermophysical properties, entropy generation and convective heat transfer for a nitrogen-doped graphene nanofluid in a laminar flow regime. Adv Powder Technol 2016; 27(2): 717-727.

[50] Vo DD, Alsarraf J, Moradikazerouni A, Afrand M, Salehipour H, Qi C. Numerical investigation of γ-AlOOH nano-fluid convection performance in a wavy channel considering various shapes of nanoadditives. Powder Technol 2019; 345: 649-657.

[51] Mirzaei M, Dehghan M. Investigation of flow and heat transfer of nanofluid in microchannel with variable property approach. Heat Mass Transf 2013; 49(12): 1803-1811.

[52] Sun B, Yang A, Yang D. Experimental study on the heat transfer and flow characteristics of nanofluids in the built-in twisted belt external thread tubes. Int J Heat Mass Transf 2017; 107: 712-722.

[53] Sun B, Peng C, Zuo R, Yang D, Li H. Investigation on the flow and convective heat transfer characteristics of nanofluids in the plate heat exchanger. Exp Therm Fluid Sci 2016; 76: 75-86.

[54] Sun B, Lei W, Yang D. Flow and convective heat transfer characteristics of Fe_2O_3-water nanofluids inside copper tubes. Int Commun Heat Mass Transf 2015; 64: 21-28.

[55] Sheikholeslami M, Ganji DD. Heat transfer improvement in a double pipe heat exchanger by means of perforated turbulators. Energy Convers Manage 2016; 127: 112-123.

[56] Sheikholeslami M, Bhatti MM. Forced convection of nanofluid in presence of constant magnetic field considering shape effects of nanoparticles. Int J Heat Mass Transf 2017; 111: 1039-1049.

[57] Sheikholeslami M. Magnetohydrodynamic nanofluid forced convection in a porous lid driven cubic cavity using Lattice Boltzmann method. J Mol Liq 2017; 231: 555-565.

[58] Sheikholeslami M, Hayat T, Alsaedi A. Numerical simulation of nanofluid forced convection heat transfer improvement in existence of magnetic field using lattice Boltzmann method. Int J Heat Mass Transf 2017; 108: 1870-1883.

[59] Sheikholeslami M, Vajravelu K. Forced convection heat transfer in

Fe_3O_4-ethylene glycol nanofluid under the influence of Coulomb force. J Mol Liq 2017; 233: 203-210.

[60] Sheikholeslami M, Hayat T, Alsaedi A, Abelman S. Numerical analysis of EHD nanofluid force convective heat transfer considering electric field dependent viscosity. Int J Heat Mass Transf 2017; 108: 2558-2565.

[61] Ranjbarzadeh R, Karimipour A, Afrand M, Isfahani AHM, Shirneshan A. Empirical analysis of heat transfer and friction factor of water/graphene oxide nanofluid flow in turbulent regime through an isothermal pipe. Appl Therm Eng 2017; 126: 538-547.

[62] Moradikazerouni A, Afrand M, Alsarraf J, Mahian O, Wongwises S, Tran MD. Comparison of the effect of five different entrance channel shapes of a micro-channel heat sink in forced convection with application to cooling a supercomputer circuit board. Appl Therm Eng 2019; 150: 1078-1089.

[63] Dehghan M, Valipour M S, Saedodin S. Microchannels enhanced by porous materials: heat transfer enhancement or pressure drop increment?. Energy Convers Manage 2016; 110: 22-32.

[64] Dehghan M, Daneshipour M, Valipour MS. Nanofluids and converging flow passages: A synergetic conjugate-heat-transfer enhancement of micro heat sinks. Int Commun Heat Mass Transf 2018; 97: 72-77.

[65] Nojoomizadeh M, Karimipour A, Firouzi M, Afrand M. Investigation of permeability and porosity effects on the slip velocity and convection heat transfer rate of Fe_3O_4/water nanofluid flow in a microchannel while its lower half filled

by a porous medium. Int J Heat Mass Transf 2018; 119: 891-906.

[66] Moradikazerouni A, Afrand M, Alsarraf J, Wongwises S, Asadi A, Nguyen TK. Investigation of a computer CPU heat sink under laminar forced convection using a structural stability method. Int J Heat Mass Transf 2019; 134: 1218-1226.

[67] Ranjbarzadeh R, Isfahani AM, Afrand M, Karimipour A, Hojaji M. An experimental study on heat transfer and pressure drop of water/graphene oxide nanofluid in a copper tube under air cross-flow: applicable as a heat exchanger. Appl Therm Eng 2017; 125: 69-79.

[68] Biglarian M, Gorji MR, Pourmehran O, Domairry G. H_2O based different nanofluids with unsteady condition and an external magnetic field on permeable channel heat transfer. Int J Hydrogen Energ 2017; 42(34): 22005-22014.

[69] Naphon P, Wiriyasart S. Pulsating flow and magnetic field effects on the convective heat transfer of TiO_2-water nanofluids in helically corrugated tube. Int J Heat Mass Transf 2018; 125: 1054-1060.

[70] Naphon P, Wiriyasart S. Experimental study on laminar pulsating flow and heat transfer of nanofluids in micro-fins tube with magnetic fields. Int J Heat Mass Transf 2018; 118: 297-303.

[71] Naphon P, Wiriyasart S, Arisariyawong T. Artificial neural network analysis the pulsating Nusselt number and friction factor of TiO_2/water nanofluids in the spirally coiled tube with magnetic field. Int J Heat Mass Transf 2018; 118: 1152-1159.

[72] Naphon P, Nakharintr L, Wiriyasart S. Continuous nanofluids jet impingement

heat transfer and flow in a micro-channel heat sink. Int J Heat Mass Transf 2018; 126: 924-932.

[73] Zhai X, Qi C, Pan Y, Luo T, Liang L. Effects of screw pitches and rotation angles on flow and heat transfer characteristics of nanofluids in spiral tubes. Int J Heat Mass Transf 2019; 130: 989-1003.

[74] Mei S, Qi C, Luo T, Zhai X, Yan Y. Effects of magnetic field on thermo-hydraulic performance of Fe_3O_4-water nanofluids in a corrugated tube. Int J Heat Mass Transf 2019; 128: 24-45.

[75] Wang G, Qi C, Liu M, Li C, Yan Y, Liang L. Effect of corrugation pitch on thermo-hydraulic performance of nanofluids in corrugated tubes of heat exchanger system based on exergy efficiency. Energy Convers Manage 2019; 186: 51-65.

[76] Qi C, Wan YL, Li CY, Han DT, Rao ZH. Experimental and numerical research on the flow and heat transfer characteristics of TiO_2-water nanofluids in a corrugated tube. Int J Heat Mass Transf 2017; 115, 1072-1084.

[77] Qi C, Liu M, Luo T, Pan Y, Rao Z. Effects of twisted tape structures on thermo-hydraulic performances of nanofluids in a triangular tube. Int J Heat Mass Transf 2018; 127: 146-159.

[78] Qi C, Liu M, Tang J. Influence of triangle tube structure with twisted tape on the thermo-hydraulic performance of nanofluids in heat-exchange system based on thermal and exergy efficiency. Energy Convers Manage 2019; 192: 243-268.

[79] Qi C, Wang G, Yan Y, Mei S, Luo T. Effect of rotating twisted tape on

thermo-hydraulic performances of nanofluids in heat-exchanger systems. Energy Convers Manage 2018; 166: 744-757.

[80] Qi C, Yang L, Chen T, Rao Z. Experimental study on thermo-hydraulic performances of TiO_2-H_2O nanofluids in a horizontal elliptical tube. Appl Therm Eng 2018; 129: 1315-1324.

[81] Ehyaei MA, Rosen MA. Optimization of a triple cycle based on a solid oxide fuel cell and gas and steam cycles with a multiobjective genetic algorithm and energy, exergy and economic analyses. Energy Convers Manage 2019; 180: 689-708.

[82] Hosseinpour J, Sadeghi M, Chitsaz A, Ranjbar F, Rosen MA. Exergy assessment and optimization of a cogeneration system based on a solid oxide fuel cell integrated with a Stirling engine. Energy Convers Manage 2017; 143: 448-458.

[83] Moharramian A, Soltani S, Rosen MA, Mahmoudi SMS, Bhattacharya T. Modified exergy and modified exergoeconomic analyses of a solar based biomass co-fired cycle with hydrogen production. Energy 2019; 167: 715-729.

[84] Rose JW. Heat-transfer coefficients, Wilson plot and accuracy of thermal measurements. Exp Therm Fluid Sci 2004; 28(2-3): 77-86.

[85] Gnielinski V. New equations for heat and mass-transfer in turbulent pipe and channel flow. Int Chem Eng 1976; 16(2): 359-368.

[86] Pak BC, Cho YI. Hydrodynamic and heat transfer study of dispersed fluids with submicron metallic oxide particles. Exp Heat Transfer Int J 1998; 11(2): 151-170.

[87] Kline SJ. Describing uncertainty in single sample experiments. Mech Eng 1953; 75: 3-8.

[88] Qi C, Liang L, Rao Z. Study on the flow and heat transfer of liquid metal based nanofluid with different nanoparticle radiuses using two-phase lattice Boltzmann method. Int J Heat Mass Transf 2016; 94: 316-326.

[89] Ma L, Yang J, Liu W, Zhang X. Physical quantity synergy analysis and efficiency evaluation criterion of heat transfer enhancement. Int J Therm Sci 2014; 80: 23-32.